Assessment of two intense dust storm characteristics over Indo – Gangetic basin and their radiative impacts: A case study

Shani Tiwari, Akhilesh Kumar, Vineet Pratap, A.K. Singh

PII: S0169-8095(18)31679-X
DOI: https://doi.org/10.1016/j.atmosres.2019.05.011
Reference: ATMOS 4581

To appear in: *Atmospheric Research*

Received date: 31 December 2018
Revised date: 5 May 2019
Accepted date: 14 May 2019

Please cite this article as: S. Tiwari, A. Kumar, V. Pratap, et al., Assessment of two intense dust storm characteristics over Indo – Gangetic basin and their radiative impacts: A case study, Atmospheric Research, https://doi.org/10.1016/j.atmosres.2019.05.011

Assessment of two intense dust storm characteristics over Indo – Gangetic Basin and their radiative impacts: a case study

Shani Tiwari[1,2#], Akhilesh Kumar[1], Vineet Pratap[1], A. K. Singh[1,3#]

[1]*Atmospheric Research Laboratory, Department of Physics, Banaras Hindu University, Varanasi, India, 221005*

[2]*Now at Environmental Research Institute, Shandong University, Qingdao, China*

[3]*DST - Mahamana Centre of Excellence in Climate Change Research, Banaras Hindu University, Varanasi, India.*

Abstract:

The present study is focused to examine the impacts of two intense dust storms on aerosol characteristics and their **radiative impacts** occurred in pre-monsoon season of 2018 (i.e. 17 May and 14 June 2018) over Kanpur (26.51^0 N, 80.23^0 E, 123 above msl). Moderate Resolution Imaging Spectroradiometer (MODIS) true colour images, trajectory pathways of dust storm along with satellite observation and AErosol RObotic NETwork (AERONET) measurements confirms that both the dust storms are either originated from or transported over the Thar Desert, causing a higher aerosol loading which spread over entire **Indian-Gangetic Basin** (IGB) and modifying the aerosol optical (i.e. aerosol optical depth, angstrom exponent, refractive index etc.), physical (i.e. size distribution) and radiative properties (i.e. single scattering albedo, asymmetric parameter). The space-borne Cloud-Aerosol Lidar and Infrared Pathfinder Satellite Observation (CALIPSO) - retrieved aerosol measurements reveal the presence of elevated dust/polluted dust aerosol (up to 3 – 5 km) over IGB which is well corroborated with aerosol characteristics observed by MODIS, Ozone Monitoring Instrument (OMI) and Atmospheric Infrared Sounder (AIRS). The Dust Regional Atmospheric Model (DREAM8b) shows a good agreement with satellite retrievals with higher value of surface dust concentration in the range of 320 – 640 $\mu g/m^3$ over Kanpur during the dust storm days. An enhancement in monthly mean outgoing longwave radiation (up to 60 Wm^{-2}) is observed over IGB and downwind flow region during the dust storm days. The atmospheric aerosol radiative

forcing is found 124 Wm^{-2} and 84 Wm^{-2} during both the dust storm days (17 May and 14 June 2018) associated with heating rate 2.69 K day^{-1} and 1.84 K day^{-1} respectively which may be significant to affect the regional atmospheric dynamics and hence the climate system also.

#Correspond to:

Dr. Shani Tiwari
Environmental Research Institute
Shandong University, Qingdao, China
Email: pshanitiwari@gmail.com

Dr. Abhay Kumar Singh
Atmospheric Research Lab., Department of Physics, Banaras Hindu University, Varanasi,
Email: abhay_s@reiffmail.com

1. Introduction:

Dust is one of the most important constitutes of aerosol loading and contributes nearly 75% global aerosol mass load and 30% of global aerosol optical thickness (Wang et al., 2015; Kinne et al., 2006). **The global climate models also suggest the higher value of total global dust emission (~ 500 – 6000 Tg/year), which are mainly associated with a large uncertainty due to different source region, transportation and complex atmospheric conditions (Huneeus et al., 2011; Prospero et al., 2010).** They are removed from the atmosphere through dry deposition (coarser particles: > 2μm diameter, near the source region) and wet deposition (fine particles, due to the long – range transport over the oceanic region). **Dust aerosols have ability to perturb the Earth's radiation budget through their direct (scattering as well as absorbing of solar and terrestrial thermal radiation), indirect (modification of cloud optical properties and lifetimes) and semi – direct effects (changing the evaporation rate of cloud droplets)** (Kedia et al., 2018; Seinfeld et al., 2016; Altaratz et al., 2014; Piedeherro et al., 2014; Obregon et al., 2015). Recently it has been found that dust aerosols can also influence the atmospheric dynamics, hydrologic cycle, monsoon system (Kedia et al., 2018; Sharma et al., 2017; Kaskaoutis et al., 2014; Vinoj et al., 2014; Kim et al., 2011;

Mahowald, 2011). Many studies have reported that the dust aerosols cause not only delay in the onset but also weakens the East Asian Summer Monsoon (EASM) (Guo and Yin, 2015; Sun et al., 2012; Ramanathan et al., 2005) while some other also reported that dust aerosol can strengthen the Indian Summer Monsoon (ISM) system by heating the troposphere (Solmon et al., 2015; Jin et al., 2014; Vinoj et al., 2014). Apart from these, dust aerosols can also affect the air quality, atmospheric chemistry, vegetation, public health and welfare, (Carugno et al., 2016; Raspanti et al., 2016; Singh et al., 2016; Singh and Dey, 2012; Dey et al., 2004). The dust particles are well mixed with fine mode anthropogenic aerosols (Tiwari et al., 2016a: Srivastava and Ramachandran, 2013) resulting a thick aerosol layer, also known as atmospheric brown carbon which have a serious implication on the Earth's biosphere, cryosphere and eco-system (Gautam et al., 2013; Ramanathan et al., 2005). During the last decade, several studies have been carried out throughout worldwide to understand anomalous behaviour of dust aerosols and their **radiative** impacts (Kedia et al., 2018; Singh et al., 2016), however a large uncertainties are still remaining (Kedia et al., 2018; Kaskaoutis et al., 2016; Singh et al., 2016; Kumar et al., 2015; Tiwari et al., 2015; IPCC 2013; Kim et al., 2011) mainly because of the complexity in dust size distribution, morphology and chemical composition (IPCC 2013; Kim et al., 2011; Lafon et al., 2006). Thus**,** the assessment of the characteristics of dust aerosol is the challenging issues due to different complex non- liner interaction between dust, meteorological condition, solar radiation and clouds (IPCC 2013).

Dust storms often occur over arid and desert regions when the strong wind blows loose sand from a dry surface and injected abundance of dust aerosols in to the atmosphere (Crosbie et al., 2014; Ginoux et al., 2012). Depending on the wind intensity, it transported thousands of kilometer**s** horizontally passing through one continent to another continent and vertically up to 6 – 8 km (Tan et al., 2017; Kaskaoutis et al., 2014; Nastos, 2012). Indo - Gangetic Basin (IGB) is one of the largest river basins in the world, experience dust storm frequently during pre-monsoon season (April - June) which carry a large amount of dust aerosol resulting enhancement in aerosol optical depth which is

more than two fold and reduce the solar radiation nearly 50 – 100 **W**m^{-2} at the surface (Singh et al., 2016; Kumar et al., 2015; Singh, and Beegum, 2013; Pandithurai et al., 2008). During pre-monsoon season, the dry weather condition and prevailing westerly/southwesterly winds in lower atmosphere supports the maximum dust transportation over IGB from the Middle East, Thar Desert and Southwest Asia (Kedia et al., 2018; Singh et al., 2016; Tiwari et al., 2015, 2013; Kaskaoutis et al., 2014). The synoptic meterological condition during the pre-monsoon season of 2018 over Indian subcontinent is shown in Figure 1 using National Centre for Environmental Prediction (NCEP) – National Centre for Atmospheric Research (NCAR) reanalysis average data of weather parameters such as wind, air temperature, and relative humidity (RH) at 850 hPa pressure level. Winds are shown with arrows pointing towards the wind direction, where the length of arrows defines the magnitude of wind speed (in meters per second), shaded color contour represents RH (%), showing red color for high and violet/blue color for low RH, and line contour represents air temperature (in K). Results reveal that the study regions are generally characterized by westerly to north-westerly winds passing through the arid region, carry higher ammount of miniral dust over IGB. A positive gradient **in** RH is also observed from western to eastern IGB indicating relatively dry air mass over western IGB. The average air temprature does not show a significant variation and lie in between 296 – 300 K over the region duriing pre-monsoon season. Similar results are also observed by Tiwari et al. (2013) and Srivastava et al. (2011) over IGB during the pre-monsson season.

Satellite remote sensing is well accepted and widely used for the detection, mapping of dust storms and their transportation and ample studies have been carried out to investigate the dust storms characteristics using this technique worldwide (Namdari, et al., 2018; Mandija et al., 2017; Tang et al., 2015; El-Askary 2015; 2006; Kaskaoutis et al. 2007; Dey et al. 2004). However, the limitations of satellite remote sensing (like spatial distribution, cloud contamination and data retrievals algorithm etc.), reflectance properties of dust and density of dust plumes, causes large uncertainty in providing accurate information about dust storms. Therefore, combined used of satellite remote

sensing along with ground based measurements of dust aerosol properties in aggregation with meteorological (e.g. wind speed, wind direction, visibility and geopotential height etc.) and modeled data is widely used over IGB by earlier researchers (Singh et al., 2016; Kumar et al., 2015; Srivastava et al., 2014; Pandithurai et al., 2008; Sharma et al., 2012; Badarinath et al. 2010; Gautam et al., 2009; Dey et al., 2004). The study of dust aerosol characteristics is highly needed over IGB since dust are mixed with anthropogenic aerosol and affect the radiative forcing of the atmosphere (Singh et al., 2016; Tiwari et al. 2015; 2016a; Srivastava et al. 2012a). With this facet, Prasad and Singh (2007) performed a long term (2001 - 2005) dust storm characteristics over IGB using ground and satellite data while others were only focused only on selected dust storms and estimated the aerosol radiative forcing during these events over Patiala (Singh et al., 2016; Sharma et al., 2012), Delhi (Singh and Beegum 2013; Pandithurai et al., 2008), Kanpur (Kumar et al., 2015; Srivastava et al., 2014; Gautam et al., 2009), over the Gangetic–Himalayan region by Srivastava et al. (2011) and over the Western Ghats (Aher et al., 2014). Elevated dust loadings (up to 4 km) over the IGB are reported during the pre-monsoon seasons (Prospero et al., 2002) which also extend over downwind region up to Bay of Bengal (Tiwari et al., 2016a). An enhancement in columnar water vapour during dust events is also reported (Singh et al., 2016; Kumar et al., 2015; Prasad and Singh, 2007) which may also increase radiative heating subject to net atmospheric warming (Kim, 2004).

In the present study, we have considered two major dust storm events (16 – 18 May and 13–14 June 2018) that occurred recently during pre-monsoon season 2018, over the IGB, to investigate their influence on aerosol optical properties, vertical profiles, aerosol radiative forcing (ARF). NCEP/NCAR reanalysis data is used for the study of the synoptical meteorological condition while the NOAA HYSPLIT model is used to track the transported pathways of dust storms. The aerosol properties and atmospheric radiative forcing are analysed over Kanpur (26.51^0 N, 80.23^0 E, 123 above msl), located in central IGB, using **ground-based** AErosol RObotic NETwork (AERONET)

data while satellite remote sensing is used for study of modification in aerosol loading during the transportation of dust storm and their vertical distribution.

2. Instrumentation and Data Analysis

2.1. AErosol RObotic NETwork (AERONET)

In the present study, the aerosol characteristics during the dust events are observed using **ground-based** observation by CIMEL sun/sky radiometer measurements data which is installed at Kanpur under AERONET program of NASA, USA. The direct sun measurements are made at eight different wavelengths within the range from 0.34 – 1.02 μm (0.34, 0.38, 0.44, 0.50, 0.67, 0.87, 0.94, and 1.02 μm) which provide the aerosol optical depth (AOD) and columnar water vapour (only at 0.94 μm) with triplet observation per wavelength. In addition, it also measures diffuse sky radiance at four spectral bands centered at 0.44, 0.67, 0.870, and 1.02 μm which is used to retrieve aerosol columnar volume size distribution (AVSD), phase function, asymmetry parameters (AP), refractive indices of aerosols and single scattering albedo (SSA) by following inversion method (Dubovik and King, 2000; Holben et al., 1998). Further details of the retrieval accuracy from the sun and sky radiance measurements are also discussed elsewhere (Dubovik et al., 2000). The processed data are available online in three different versions (1, 2 and 3) with three different categories viz. (a) cloud contaminated (level 1.0), (b) cloud screened (level 1.5) and (c) quality assured (level 2.0). In the present study, version 2, level 1.5 data is used, which is only available dataset for all the parameters. This level data is also used previously by others (Tiwari et al., 2013; Srivastava et al., 2011; Prasad et al., 2007) and the deviation of Level 1.5 AOD value from level 2.0 is found within the range of 0 - 5% over IGB (Tiwari et al., 2013).

The uncertainty in AOD calculation under cloud free condition is less that ±0.01 for higher wavelengths ($\lambda > 0.44$ μm) and less than ± 0.02 for shorter wavelengths; while columnar water vapor has uncertainties up to 10% (Dubovik et. al., 2000; Eck et. al., 1999). Relatively higher uncertainties

(10 - 15%) are observed for AOD_{440} > 0.4 for sky radiance measurements (Dubovik and King, 2000; Dubovik et al., 2000, 2002). The errors are not significant for the particles of radius (R) in the range 0.1–7 μm. The tendency for increasing errors in retrieval of optical properties with the decrease in optical depth is higher in the case of refractive index **(RI)** and single scattering albedo **(SSA)** than in the case of volume size distribution (Dubovik et al., 2000). However, these errors do not significantly affect the important characteristic features of the size distribution (Dubovik et al., 2000).

2.2. *Moderate Resolution Imaging Spectroradiometer (MODIS)*

In addition to the ground observed AERONET data, MODIS level 3 collection C006.1 AOD (at 550 nm) data on board of **Terra** satellite is used over the IGB during the dust events. It measures the radiance at 36 spectral bands in the visible to thermal IR spectral range of 0.41–14 μm (Kaufman et al., 1997) and has a wide swath of 2330 km which makes it possible to observe global data in a single day. It passes over the Indian region at ~10:30 am (Terra) and ~01:30 pm (Aqua) local solar time. The aerosol properties are retrived between the spectral bands 0.4 to 2.1 μm using different algorithm over land (three wavelengths band) and oceanic regions (seven wavelength bands) (Kumar et al., 2009; Prasad and Singh, 2009; Remer et al., 2005). The uncertainity in AOD measurement over ocanic regions is relatively higher i.e. ± (0.03 ± 0.05 τ) than over the land i.e. ± (0.05 ± 0.15 τ) (Tiwari et al., 2016a; Prijith et al., 2013; Levy et al., 2010; Remer et al., 2005). Several researchers widely used MODIS dataset and images to identify the dust storms and their transportation (Singh et al., 2016; Kumar et al, 2015; Sharma et al., 2012; Badarinath et al., 2010; Hsu et al., 2006). Images of dust storms are downloaded from the site (https://lance-modis.eosdis.nasa.gov/cgi-bin/imagery/realtime.cgi). Details about instrumentations, algorithms and error estimations are described by Kaufman and Tanre (1998), and updates are discussed by Remer et al. (2005).

2.3. Ozone Monitoring Instrument (OMI)

Along with MODIS – AOD data, UV Aerosol Index (AI) values obtained from the Ozone Monitoring Instrument (OMI) on board the Finnish–Dutch Aura satellite are used. It was designed to replace the Total Ozone Mapping Spectrometer (TOMS) to continue recording total ozone and other atmospheric parameters related to atmospheric chemistry and climate. The OMI is a nadir viewing, having wide swath with twenty hyperspectral imaging spectrometer that provides daily global coverage with high spectral resolutions and spatial resolution of 13 km × 24 km at nadir **and also capable to detect the aerosol above the cloud (Levelt et al., 2006).** It takes advantage of the greater sensitivity of radiances measured at the troposphere in the near UV region to the varying load and type of aerosols to derive Extinction Aerosol Optical Depth (EAOD), Single Scattering Albedo (SSA) and Absorbing Aerosol Optical Depth (AAOD) using an inversion procedure at 354, 388 and 500 nm generated by the near UV (OMAERUV) algorithm (Torres et al., 2007). It assumes that the column aerosol load can be represented by one of three types of aerosols and uses a set of aerosol models to account for the presence of these aerosols: carbonaceous aerosols from biomass burning, desert dust, and light absorbing sulfate based aerosols. For carbonaceous and desert dust particles, the aerosol loading is assumed to be vertically distributed following a Gaussian function characterized by peak (aerosol layer height) and half-width (aerosol layer geometric thickness) values (Torres et al., 2013). The AI is defined as the difference between measured (including aerosol effects) spectral contrast at 331 and 360 nm wavelength radiances and the contrast calculated from the radiative transfer theory for a pure molecular (Rayleigh particles) atmosphere (Curier et al., 2008) and highly sensitive to miniral dust, carbonaceous aerosol and aerosol layer height also (Singh et al., 2016; Tiwari et al., 2016a; Eck et al., 2001; Hsu et al., 1999). In the present study, level 3 global – gridded products (with 0.25° × 0.25 ° spatial resolutions) OMI UV – AI value is used during dust events to evaluate the dust – source region and the transportation. The positive value of AI indicates the presence of UV absorbing aerosols, like dust, smoke whereas the negative value

indicates the presence of non-absorbing aerosols like sulphate (Singh et al., 2016; Kaskaoutis et al., 2010).

2.4. Cloud-Aerosol Lidar and Infrared Pathfinder Satellite Observation (CALIPSO)

The vertical profile of dust aerosols is very important because of their **crucial** role in calulation of atmospheric radiative forcing and heating rate (Lemaitre et al., 2010). In this aspect, the space lidar, Cloud-Aerosol Lidar and Infrared Pathfinder Satellite Observations (CALIPSO) provides a new perceptions into the monitoring of atmospheric dust, their transport, and vertical extent and widely used worldwide (Proestakis et al., 2018; Filonchyk et al., 2018; Tiwari et al., 2016a; Kumar et al., 2015; Liu et al., 2012; Mishra and Shibata, 2012; Kaskaoutis et al., 2012). CALIPSO's orbit has a 16 – day repeat cycle, which produces sub-satellite tracks spaced longitudinally by 172 km at the equator. However, as CALIPSO observations are limited to the sub-satellite track, its spatial coverage is very poor compared to MODIS. CALIOP can observe aerosol over bright surfaces and beneath thin clouds as well as under clear sky conditions while it can not provide observations at altitude regions that are below optically thick clouds. In this study, CALIOP level 2 Ver. 3.01 data product (Young and Vaughan, 2008) is used during dust event to understand the vertical distribution of dust aerosol. More details about the CALIPSO algorithm and it's description are described by Winker et al. (2006) and Labonne et al. (2007).

2.5. Atmospheric Infrared Sounder (AIRS)

AIRS is one of the six instruments aboard on Aqua satellites, which is a part of NASA's sun-synchronous "A Train" satellite which designed to make long – term global observations of the land surface, biosphere, solid Earth, atmosphere, and oceans from space. It has a large spectral channel (2378) spectrometers covering infrared wavelength (3.7 – 15.4 μm) and provides the accurate information about the vertical profile of atmospheric temperature, moisture. It also measures longwave radiation along with greenhouse gases such as ozone, carbon monoxide, carbon dioxide,

and methane. The outgoing longwave radiation (OLR) is highly dependent on vertical distribution of the trace gases (Susskind et al., 2012). In the present study, AIRS version 6.0, the daily mean value of OLR (daytime) with a resolution of 1° × 1° on latitude - longitude grid is used.

2.6. Meteorological Data and Hysplit Backtrajectories model

The synoptic meteorological conditions such as temperature, winds, relative humidity, geopotential height etc., play a vital role in dust storm occurance, intensity and their intercontinental transportation due to air – mass types, advection and other complex process (Singh et al., 2016; Sreekanth and Kulkarni, 2013; Satheesh et al., 2006). Thus to examine the role of synoptic meteorological conditions on aerosol transport and their distribution during the dust events, National Center for Environmental Prediction (NCEP)/National Centre of Atmospheric Research (NCAR) reanalysis data of wind vector, relative humidity and air temprature at 850 hPa is used. Five days air mass back trajectories is also computed at three different altitudes at 1000, 1500, 2000 m above mean sea level at receptor site based on National Oceanic and Atmospheric Administration (NOAA) Hybrid Single Particle Lagrangian Integrated Trajectories (HYSPLIT) model (website http://ready.arl.noaa.gov/HYSPLIT.php) using NCEP reanalysis wind data as input (Draxler and Rolph, 2003). It provides a three-dimensional (latitude, longitude, and altitude) information abouth the air mass pathways as a function of time.

2.7. BSC - DREAM model simulations

Although a significant progress has been achieved in undestading of physical and optical properties as well as the importance of mineral dust in global-scale processes (Seinfeld et al., 2016; Mahowald, 2011; Prospero et al., 2010; Lau et al., 2006; Ramanathan et al., 2005) yet the identification of atmospheric porcesses and meterological factors that affecting the dust generation near the source region, their carriage and deposition is still highly uncertain. DREAM (Dust Regional Atmospheric Modeling) is a regional 3D model designed to simulate all major processes of

the atmospheric cycle of mineral dust aerosol by solving the Euler-type partial differential non-linear equations for dust mass continuity (Nickovic et al., 2001**) and the simulations using the model are provided by the Barcelona Supercomputing Center (BSC), hence called BSC-DREAM model.** The near-surface wind, thermal conditions, and soil features along with surface elevation, soil properties, turbulent mixing and vegetation cover are used for the simulation of the dust production. The model configures four dust particle size classes (clay, small silt, large silt, and sand) with particle size radii of 0.73, 6.1, 18 and 38 μm, respectively. For the analysis of long-range transport, only the first two dust classes are relevant since their atmospheric life time is greater than about twelve hours (Perez et al., 2006) and these particles can be transported over long distances whereas the latter two are deposited near the dust source region. **The model has the capability to predict and forcast almost every major dust storms (Pérez et al., 2006; Amiridis et al., 2009) and validated with earlier studies under different programs worldwide like the EARLINET (European Lidar Network), the AERONET sunphotometer network as well satellite observations also (Haustein et al., 2009; Todd et al., 2008; Perez et al., 2006).**

3. Results and Discussion:

3.1. Satellite observation and dust storm characteristics:

Two intensive dust events were observed during May (17 – 18) and June (13 – 14), 2018 over entire IGB which **reduced** the atmospheric visibility, air quality and atmospheric ventilation coefficient over the entire region, causes adverse impacts on human health. One of the major reasons of such severe dust storm can be ascribed to the convergence of two different fronts, strong convection which carried enormous dust aerosol from the Middle East and the Thar Desert (Kaskaoutis et al., 2018; Singh et. al., 2016; Kumar et al., 2014; Singh and Beegum, 2013). Figure 2 shows MODIS aqua true colour image during the dust events, which clearly show an intense dust

plumes (pale colour) over the Thar Desert and moving towards IGB on 17 June 2018, however relatively more intense dust plume can be seen over IGB which initially moving to the northeast direction and then towards southeast with a slightly negative gradient in its thickness. **The propagation of dust plumes towards the northeast deposit the plenty of dust over the Himalayan foothills region which strongly affects the radiative balance over the region** (Bucci, et al., 2014; Gautam et al., 2013, 2009**).** The transportation of dust plumes and its intensity, uplift is highly influenced by local and regional meteorology (Singh et al., 2016; Kumar et al., 2015, 2014; Gharai et al., 2013; Badarinath et al., 2010). The **long-range** transportation of the dust plumes from the Middle East and the Thar Desert region is also supported by the five days air mass back trajectories at three different altitudes (viz. 1000, 1500 and 2000 m above ground level). On 17 May 2018, the air masses are mainly coming from the Arabian Peninsula (AP) at the lower altitude (1000 m) while at higher altitude (1500 and 2000), mainly from the Middle East region passing through the AP (Figure 3a). On the other hand, during other dust storm day (14 June 2018) air masses at Kanpur are mainly coming from the Middle East region, passing through the AP and Thar Desert resulting in to higher concentration aerosol over entire IGB. Earlier studies also reported the **long-range** transportation and enhancement in aerosol loading over IGB during dust events (Bran et al., 2018; Kedia et al., 2018; Yadav et al., 2017; Singh et al., 2016; Kumar et al., 2015, 2014; Singh and Beegum, 2013; Badarinath et al., 2010; Pandithurai et al., 2008; Dey et al., 2004). The enhancement in aerosol loading over IGB is also clearly depicted from the spatial distribution of aerosol optical depth (AOD) during the dust events (Figure 3a and 3b), obtained from MODIS on board of Terra satellite. The colour scale represents AOD value while white patches show the absence of data. Highest AOD is obtained over IGB during both the dust events with relatively higher concentration during the second event (14 June 2018). A small negative gradient in AOD is also observed from western to eastern IGB suggesting the decreasing pattern of dust deposition concentration from western to eastern IGB and also further confirmed the decrease in thickness of dust plumes as it

moving towards the southeast direction, which is already discussed earlier. A negative gradient in aerosol loading from western to eastern IGB is also reported by earlier researcher**s** during **different** dust events and pre-monsoon season (Kedia at al., 2018; Bran et al., 2017; Singh et al., 2016; Srivastava et. al., 2014; Kumar et al., 2015, 2014; Tiwari et al., 2013). To understand the impact of these dust events on AOD loading, we calculated the enhancement factor (EF) for each grid points, which is the ratio of AOD difference between AOD on dusty days and monthly/seasonal mean AOD to monthly/seasonal mean AOD (i.e. EF = ($AOD_{dusty\ days}$ – monthly / seasonal mean AOD)/ monthly/seasonal mean AOD). The spatial distribution of EF suggest**s** the enhancement in aerosol loading over the region in a factor of more than two (Figure 4) which not only affect the monthly mean aerosol loading but also on a seasonal basis, causes a significant uncertainty in atmospheric radiative forcing and global climate model. Figure 4, suggest that relatively lower EF on monthly (4a) and seasonal basis (4c) during the first dust events which enhance the AOD loading not only over **the** IGB but also **over the** northern Arabian sea (AS), central, south central India and downwind flow region (northern Bay of Bengal: BOB) suggesting the occurrence long range transport of dust mainly because of suitable meteorological conditions. Recently Tiwari et al. (2016a) also observed elevated dust aerosol and increase in aerosol loading during pre-monsoon season over AS and BOB which are coming from the Middle East region through long range transportation. Apart from this, a large EF (up to two) is observed due to second dust storm (14 June, 2018) which is more prominence on a seasonal basis (4d) rather than on monthly (4b) suggesting relatively higher AOD during June month mainly because of frequent occurrence of dust storm over **the** Thar Desert and AS (Kumar et al., 2015; Kaskaoutis et al., 2014). Earlier studies also reported higher AOD value during **the month of** June, mainly coming from the arid regions through AS (Tiwari et al., 2016a; Kumar et al., 2015; Kaskaoutis et al., 2014; Prijith et al., 2013). The highest value of EF during pre-monsoon season over **the** Thar Desert region suggest the major contribution of dust aerosol loading is from this region during the second dust storm. Earlier researchers also found the Thar Desert region as the major

contributor of dust aerosol during the dust storms (Singh et al., 2016; Kumar et al., 2015; Srivastava et al., 2014).

In conjugation with AOD, Aerosol Index (AI) provides valuable information about the absorbing aerosol (e.g. dust aerosol or smoke). Figure 5 shows the spatial distribution of AI during dust events i.e. (a) 16 May, 2018 (due to unavailability of data) and (b) 14 June, 2018. Figures (both 5(a) and 5(b)) clearly suggest the presence of dust over IGB, northern AS and western part of India and outlines the transport of dust plumes. In both the figures, higher values of AI are qualitatively agreed with MODIS AOD and dust transportation. The AI value ranging from 1.5 – 4 over IGB represent the dust spreading over entire **the** IGB during dust events which are further confirmed by the higher AI value (>1.7) in the conjugation of higher AOD value (>1.0) during events. Recently Singh et al. (2016) also reported higher AI value (2.0 – 2.5) associated with higher AOD (>0.9) during an unusual dust storm event occurred in March 2012 over IGB, however, Sharma et al. (2012) found relatively higher range of AI value (2.0 – 6.7) during an intense dust storm occurred in April 2010. On 14 June 2018, AI values are nearly double (>3.0) over IGB than 17 May 2018 which confirm the more intense dust event. The AI image (Figure 5b) in combination with trajectories and AOD image (Figure 3b), clearly indicate that the dust originated from the Thar Desert have the maximum contribution of dust loading over IGB on 14 June, 2018. Higher value of AI (>3.0) on 14 June 2018, also indicates the existence of elevated dust aerosol which may be due to the strong convection, meteorological condition and the long-range transportation. Earlier studies also reported the higher AI values (>2. 5) for elevated dust aerosols (Tiwari et al., 2016a; Singh et al., 2016; Aher et al., 2014; Prijith et al., 2013; Badarinath et al., 2010; Kaskaoutis et al., 2008; Dey et al., 2004). We also calculated the enhancement factor (EF) for AI, at every grid point during the dust storm, to investigate the impact of events on dust loading and their transportation over the Indian subcontinent. The spatial distribution of EF for AI is shown in Figure (6) at monthly (a, c) as well as seasonal basis (b, d) for both the dust events respectively. Figure clearly reflects that on 17 May, 2018, highest EF

value (in the range of 1- 2) is associated with a large spatial distribution and spread over the Thar Desert, northern AS, and northern BOB which is more eminence on seasonal basis (Figure 6a and 6c) suggesting enhancement in dust loading. Recently, Tiwari et al. (2016a) also found an increase in dust aerosol loading over AS and BOB during pre-monsoon season however, Prijith et al. (2013) reported enhancement in dust loading in month of June over AS. On the other hand, maximum EF is found over IGB with an increasing pattern from western to eastern IGB during both, on June month as well as pre-monsoon season (Figure 6a and 6c) suggesting the occurrence of an intensive dust storm which uplift the dust particles at higher altitude and spread over entire IGB. Kumar et al. (2015) also found elevated dust aerosol (up to 1 – 4 km) over IGB during different dust events in pre-monsoon season of the year 2010. A similar result is also reported by Liu et al. (2011) over the Yangtze delta region, China, during intense dust storms in March and April 2009. A pocket of higher EF over coastal region of Arabian Peninsula on seasonal basis suggests the dust deposition over the region during the transportation of dust plumes.

In the presence of cloud, aerosol detection over desert by using MODIS and OMI region become highly uncertain due to surface reflectivity (Levy et al., 2007; Torres et al., 2007). In this aspect, space borne lidar is widely used to detect and confirm the position, the vertical extent of dust along with the overpass trajectory. Therefore, to corroborate above two satellite measurements, we used CALIOP lidar measurements, viz. vertical profiles of the total attenuated backscatter at 532 nm, and aerosol subtypes during the dust events i.e. (a) 18 May 2018, and (b) 14 June, 2018 which is shown in Figure 7(a) and Figure 7 (b) respectively. The CALIOP observations (data level 3.04), in terms of the total attenuated backscatter at 532 nm confirm the presence of a high aerosol dust load over IGB and reach up to 5 km during the dust storm days with higher backscatter coefficient (> 0.004) which is significant to warm mid troposphere and affect the regional climate also (Gautam et al., 2010). The aerosol subtype images also clearly confirm the dominance of dust (category 2, in yellow) and polluted dust i.e. mixing of dust with anthropogenic aerosols over (category 5, in pale colour) over

IGB region which is more prominent on 14 June 2018. Similar results are also reported by Kumar et al. (2010) over Kanpur during dust event in pre-monsoon season of the year 2010 and by Alam et al. (2014) over Karachi/Lahore during an intense dust storm occurred in March 2012.

3.2. AERONET measurements of dust storm characteristics

The physical and optical properties of aerosol particles during the dust storm events are analysed using CIMEL sun/sky radiometer measurements at Kanpur AERONET station. The impact of these two dust events on aerosol characteristics at Kanpur is discussed in upcoming sections.

3.2.1. Aerosol Physical and Optical Characteristics

Aerosol optical depth and Angstrom exponent

Aerosol optical depth (AOD) and Angstrom exponent (AE) are two main parameters to understand aerosol characteristics and can be easily calculated by the equation given by Angstrom (1964),

$$\tau_a(\lambda) = \beta . \lambda^{-\alpha} \quad (1)$$

where, $\tau_a(\lambda)$ is the wavelength micrometre, τ_a is AOD for the wavelength λ, α is angstrom exponent (AE) and β is the turbidity coefficient which is equal to columnar AOD at λ = 1 µm. The AE is a relatively good indicator of the aerosol particle size and fraction of accumulation mode (r <1 µm) - to coarse-mode (r >1 µm) particles quantitatively (Tiwari et al., 2018, 2016b). The day-to-day variation of AOD (at 500 nm) and AE (derived from the wavelength pair of 440 and 870 nm) along with columnar water vapour (secondary axis) is shown in Figure 8(a) and 8(b) for both dust events occurred in May and June 2018 respectively. The monthly mean value of AOD/AE is found 0.89 ± 0.19/0.71 ± 0.21 and 1.05 ± 0.43/0.60 ± 0.35 while water vapour is 2.82 ± 0.64, 4.21 ± 0.62 in the month of May and June respectively. During the dust event in May (on 17 May, 2018), the AOD value is reached up to 1.1 (Table 1) which enhance nearly 25% of the monthly mean AOD while the AE value decreases nearly half and reached to 0.36, which indicated towards the enhancement in

coarse more aerosol particles. Apart from this, on second dust events (14, June 2018), the AOD value enhanced nearly 2.4 times than monthly mean AOD and reached at 2.38 along with nearly zero AE value (Table 1), clearly suggesting the abundance of dust particles injection in to the atmosphere due to the intense dust storm. A drastic decrease in AE value is also reported by (Singh et al., 2005) during dust storm occurred over Delhi in April 2003. A sudden decrease in AE value is mainly because of extinction of incoming solar radiation at the visible and infrared wavelengths by dust particles, resulting in small and even negative values (Hamonou et al., 1999). Dey et al. (2004) also reported an increase in AOD more than 50% and a decrease in AE between 70 – 90% during the dust storm in May 2001 – 2002 over Kanpur. Relatively lower spectral dependency in AOD is observed on 17 May 2018 than other days in May (Figure S1(a)) suggesting the dominance of coarser particles however almost flatter AOD spectra on 13 and 14 June, 2018 (Figure S1 (b)) further confirmed the being of enormous amount of dust aerosols in to the atmosphere. Relatively less spectral dependency in AOD is also reported for polluted dust aerosol over entire IGB which is mainly because of the dominance of relative amount of coarse particles (Tiwari et al., 2015; Srivastavea et al., 2014). Figure 8 (a, and b) also shows a decrease in columnar water vapour on dust storm days which enhanced after the dust storm that may be due to the transportation of moisture from the AS. Earlier studies also found an enhancement in columnar water vapour after the dust storm events (Singh et al., 2016; Kumar et al., 2015; Prasad and Singh, 2007). During the dust storm it is found that as AOD increases, water vapour also increases by power correlation law, up to 72% (Prasad and Singh, 2007).

Aerosol Volume Size Distribution (AVSD)

The plenty of the coarse mode particles in the dust storm is the primary symptoms which easily differentiate the optical properties of dust aerosol with anthropogenic and bio-mass burning aerosol. Dust aerosols have more absorbing nature of solar and infrared wavelength as compared to the anthropogenic aerosols like sulphate. The size distribution of different aerosol types highly depends

on emission sources, composition, transportation patterns and scavenging mechanism (Tiwari et al., 2015; Eck et al., 2001). Aerosol Volume size distribution (dV/dlnr) for twenty-two bins between 0.05 and 15 μm, derived from sun/sky radiometer data using Dubovik and King (2000) approach, is used during dust events at Kanpur and shown in Figure 9 (a) and (b) during May and June respectively. Figure clearly reflect a bimodal size distribution with larger peak towards coarse mode particles (fine mode **has** very small contribution) during both the events with different magnitude of dV/dlnr indicating towards the relatively small presence of fine mode particles during dusty days which may be due to the large anthropogenic emission sources and mixing of aerosol particles. Earlier studies also reported the similar size distribution for aerosol particles over Kanpur station (Kumar et al., 2015; Kaskaoutis et al., 2014; Tiwari et al., 2013; 2015; Prasad et al., 2007; Dey et al., 2004), over Delhi (Pandithurai et al., 2008) during the major dust storms and over Karachi also (Tiwari et al., 2015, 2013; Alam et al., 2012) in pre-monsoon season. The coarse mode peak is more pronounced at the radius (μm) 2.24, during both the dust events. The daily average value of volume concentration, effective radius for both fine mode and the coarse mode is given in Table 2. Monthly average volume concentration in the coarse (V_c) and fine mode (V_f) are found to be 0.44 ± 0.09 and 0.09 ± 0.02 and 0.54 ± 0.25 and 0.07 ± 0.02 in May and June 2018, respectively. During the dust events, V_c has been found to increase significantly without much change in the effective radius at the coarse-mode ($R_{eff,c}$). The effective radius of fine mode particles ($R_{eff,f}$) is relatively larger in first event (May) rather than in June which attributed to the long range transportation of fine absorbing aerosols from the eastern part of the basin. On the other hand, the value of V_f and $R_{eff.,f}$ on 14 June, 2018, is found to nearly similar to their monthly mean value for June month suggests the minimum impact of this dust storms on the particle size distribution at the fine mode side.

Refractive Index (RI)

Refractive Index is the most fundamental optical properties of atmospheric aerosol which provide significant information about the nature of aerosol particles. It is highly dependent on chemical composition and provides information about the scattering and absorbing nature of aerosol. The higher values of a real part of the refractive index (RRI) indicate scattering type of aerosol while higher values of an imaginary part of the refractive index (IRI) represent the absorbing nature of aerosol particles (Sinyuk et al., 2003). The typical value of RRI for dust is found 1.53 ± 0.05 (Sokolik and Toon, 1999; Koepke et al., 1997) in the visible spectrum while IRI is nearly 0.006 or even less (Shettle and Fenn, 1979) reported by several models to calculate the radiative transfer. The spectral variation of real and imaginary refractive indices **is** shown in Figure 10 (a and b) and Figure 10 (c & d) respectively for first (May) and second dust events (June). The RRI value is found nearly >1.5 for both events which increase up to visible range (675 nm) and then it decreases in the infrared region. Similar, higher range of RRI is also reported during dust storm over Kanpur (Kumar et al., 2015; Prasad and Singh, 2007; Dey et. al., 2004), over Karachi (Iftikhar et al., 2018; Alam et al., 2014), and over Beijing (Zhang et al., 2017). However, IRI show spectrally decreasing pattern with value in the wide range from 0.003 - 0.017 in May and 0.0005 - 0.007 in June. The spectral decrease in IRI at a higher wavelength (λ > 440 nm) indicates the dominance of mineral dust aerosols during the dust storms and a decrease in the fraction of anthropogenic (smoke) aerosols. Relatively smaller value of IRI is observed in June than in May which is mainly because of the increased concentration of scattering particles which is also confirmed by higher SSA value in June than in May. A part from this, highest RI (for both RRI and IRI) is observed on 19 May with no spectral dependency for RRI while relatively less spectral dependency for IRI suggesting the enhancement of fine absorbing aerosol which is also supported by higher AOD value associated with relatively higher AE value (Figure 8(a)) and volume size distribution (Figure 9(a)) where peak shifted towards fine mode particles. Similar results are also reported over Kanpur during the non –

dusty days (Prasad et al., 2006). The changing behaviour of the optical state of the aerosol particles during the dust events is well supported by the SSA values. The higher AOD value along with nearly zero AE value also confirm the huge amount of aerosol loading in a coarse mode which causes the low absorption. A larger difference in RRI and a nearly similar value of IRI at the higher wavelength is attributed due to the complex mineralogy during long range transportation source region of the dust (Kubilay et al., 2003).

3.2.2. Aerosol Radiative Properties

Single Scattering Albedo (SSA)

Single Scattering Albedo (SSA) is one of the most important properties of aerosol and can provide the information about the reduction in solar and terrestrial radiation in polluted environments. It provides the details information about the scattering and absorbing characteristics of different aerosol types and is a key parameter in atmospheric radiative forcing calculation. It can easily be calculated by scattering optical thickness obtained from the normalized aerosol phase function using diffuse radiance measured at different angles (Dubovik et al., 1998) and have value in the range of zero (completely absorbing like soot/black carbon) to one (completely scattering like sulphate) and highly depend on composition and size of aerosol particles (Bergstrom et al., 2007). The spectral variation of SSA is shown in Figure 11 (a and b) during the dust events. SSA is found to be strongly wavelength dependent with a higher value (SSA > 0.9) during both the events and have spectrally increasing trend from visible to near-infrared bands which further confirm the dominance of coarse mode aerosol particles as discussed earlier sections. The increasing trend of spectral variation in SSA for dust aerosol is also reported by earlier studies over IGB (Iftikhar et al., 2018; Tiwari et al., 2015, 2013; Kumar et al., 2015; Srivastava et al., 2014; Alam et al., 2011; Gautam et al., 2011; Dey et al., 2004). A steep rise in SSA spectra from 440 nm to 675 nm clearly suggests more scattering at a higher wavelength (λ > 670 nm) because of increase in the number of coarse particles

which is also confirmed from spectral variation of AOD (Figure S1), showing higher AOD value (>1) at a higher wavelength. Recently Kumar et al. (2015) found a similar range of SSA (≤ 0.95) during different dust events occurred in pre-monsoon season over Kanpur while Iftikhar et al. (2018) has found relatively higher SSA value (≥0.98) during an intense dust storm on 5th July 2014 over Karachi. Yu et al. (2016) also found the SSA value in the range of 0.89 to 0.94 during dusty days over Beijing. The figure also reveals that the magnitude of SSA value is relatively higher in the second event (in June) than the first one (in May), representing the higher concentration of coarse mode aerosol particle in June which is also reflected from the Table 2. The spectral difference in SSA (i.e. $\Delta SSA = SSA_{1020\ nm} - SSA_{440\ nm}$) is found 0.08 and 0.06 on 17 May, 2018 and 14 June 2018 respectively, which further confirmed the **long-range** transportation of desert aerosol over the region as similar range (>0.5) of ΔSSA for mineral dust is also reported by Dubovik et al. (2002).

Asymmetric Parameter (AP)

Asymmetry parameter (AP), also known as scattering parameter, provide the information about the angular distribution of light scattering by aerosol particles, defined as the cosine averaged scattering angle, and can be calculated by the integrating over the complete scattering phase function (Pandithurai et al. 2008). It has the ability to control the aerosol contribution in radiative forcing and is widely used in various radiative transfer models. It depends on the size and composition of the particles having value in the range of +1 (for forward scattering) and −1 (for backward scattering), while zero value represents the pure symmetry scattering (Tiwari et al., 2015; Ramachandran and Rajesh, 2008; Zege et al., 1991). The spectral variation of AP during the dust events is shown in Figure 12 (a) and Figure 12 (b) for the month of May and June respectively. During both the events, AP value had decreasing spectral trend for the visible region and then a slight increase in in near infrared region with the highest value (0.71 for 17 May, 2018 and for 0.73 for 14 June, 2018) on dust storm days. Relatively small spectral slope is observed on dust storm days during both events suggesting the relative dominance of coarse mode particles. Earlier studies also reported similar

nature of spectral variation of AP for dust particles (Iftikhar et al., 2018; Tiwari et al., 2015, 2013; Alam et al., 2014; Srivastava et al., 2014; Pandithurai et al. 2008). Recently, Tiwari et al., (2015) found nearly similar value of AP for polluted dust particles over Kanpur (0.70 ± 0.02), however with little higher value (0.72 ± 0.02) over Karachi. In another study, Tiwari et al. (2013) also reported AP value nearly 0.71 ± 0.02 over Karachi, 0.68 ± 0.02 over Lahore, 0.71 ± 0.01 over Jaipur, and 0.68 ± 0.02 over Kanpur during the pre-monsoon period 2010. The results observed in the present study are quite comparable with other previous studies carried out during the dust storm over IGB (Iftikhar et al., 2018; Srivastava et al., 2014; Alam et al., 2014; Pandithurai et al., 2008).

3.3.3. Surface aerosol concentration during dust storm

The BSC- DREAM8b model simulation results have been used for dust events and to identify the dust transportation and deposition. The model results regarding the spatial distribution of dust concentration on 17 May and 14 June 2018 at 12 hrs UTC, over the Indian subcontinent and its surrounding region are presented in Figure 13(a) and 13(b) respectively. The model predicted a high surface concentration of dust in the latitudinal range from 20^0 – 38^0 N and longitudinal range 60^0 – 85^0 E with maximum surface concentration over the Thar Desert. The higher concentration of dust is also observed mainland of China which suggest that after passing through the IGB dust storm moving towards China. The wind fields at 3000 m with respect to mean sea level (see Figure S2) show that Thar Desert region is the main source region of dust storm and it is driven by westerly/north westerly winds towards the south eastern IGB. The dust deposition over IGB is higher on 14 June 2018 than 17 May 2018 which confirms the dust storm intensity and justifies the spatial variability of aerosol. The simulated surface dust concentration is found to be in the range of 320 - 640 $\mu g/m^3$ over Kanpur during both the dust events. The simulated results are also supported by the satellite observation on the same day. Relatively lower range of surface dust concentration is observed by Aher et al. (2014) over Alibag and Pune during a dust storm occurred in March 2012 while Kaskaoutis et al. (2012) reported a similar range of dust concentration over the Eastern

Mediterranean during the dust event of February 2009. Thus, the model is quite capable to predict dust storm source region and transportation of dust accurately which is also in agreement with the satellite observations **(Haustein et al., 2009; Perez et al., 2006).**

4. Radiative impacts of dust storm

4.1. Influence on outgoing long wave radiation

The outgoing longwave radiation (OLR) is one of the crucial parameters in the calculation of atmospheric radiative forcing at the top of the atmosphere and plays a significant role in atmospheric circulation pattern, hence in weather and climate prediction (Haywood et al., 2005). Atmospheric aerosols (mostly dust) have the ability to perturb the global radiation budget through the cloud radiative forcing (Zhao et al., 2018; Trenberth et al., 20009; Haywood et al., 2005; Slingo et al., 2006). Hsu et al. (2000) estimated longwave radiative forcing nearly 36 Wm^{-2} per unit optical depth using TOMS AOD over Western Sahara when the temperature was maximum. The frequent occurrence of dust storm causing an enhancement of dust aerosols in to the atmosphere resulting to a warming effect implies that the observed longwave enhancement is climatologically significant (Zhou et al., 2014). Aerosol can also cause a cooling of the atmosphere in the longwave with a relatively small contribution (~ 20%) to the net (longwave and shortwave) radiative forcing (Ramaswamy, 2002) which also increases with higher AOD value (Ramachandran and Kedia, 2012). The spatial distribution of OLR over Indian subcontinent during dust events and their impacts on monthly/seasonally mean OLR value is shown in Figure 14 (a – f). The figure clearly suggests that a higher value of OLR during both the dust events which are relatively **higher** on 14 June 2018 (Figure, 14b). Higher value of OLR is observed over the arid and desert region which may be mainly because of the dominance of dust particles which causes increasing in temperature. Earlier studies also reported higher OLR value during dust storm over the desert region (Kedia et al., 2018; Zhou et al., 2014; Hong et al., 2013, Hansell et al., 2010; Slingo, et al., 2006; Haywood et al., 2005). Apart

from this, an enhancement in OLR in monthly mean OLR is observed due to the first dust event (17 May 2018) having the range in between 10 – 20 Wm^{-2} over IGB, western Indian coast and northern AS, which may be due to less intensive dust storm resulting to lower concentration of dust aerosol than the second dust event. While it has a significant impact on seasonal OLR value over the IGB where it causes an enhancement in OLR value nearly 30 - 40 Wm^{-2}. On the other hand, second dust event (14 June, 2018) have notably impact on monthly mean OLR value in June 2018 over IGB, and central India and enhance the OLR value in the range of 50 ± 10 $\mathbf{W}m^{-2}$. The maximum enhancement in OLR is observed over south - east coastal region of India which may be due to the abundance of dust aerosol over this down flow wind region during an intense dust storm. However, the second dust event has the relatively lower impact of OLR during pre-monsoon season in 2018 with a similar pattern as in June month and enhances OLR value up to 35 Wm^{-2} over IGB. The results observed here is quite comparable with earlier studies worldwide while some discrepancy may be due to the different meteorological conditions, dust storm intensity and dust composition (Du et al., 2018; Wang et al., 2018; Zhou et al., 2014; Hong et l., 2013; Hansell et al., 2010; Slingo, et al., 2006; Haywood et al., 2005). Recently, Kedia et al. (2018) found an enhancement in OLR (~ 60 Wm^{-2}) over the Arabian Sea and some parts of central India during dust storm occurred in April 2015. Ackerman and Chung (1992) is also reported direct radiative forcing due to long wave radiation in the range of 20 – 50 Wm^{-2} over Arabian Peninsula during the Earth Radiation Budget Experiment using advanced very high-resolution radiometer (AVHRR) and model data.

4.2. Aerosol Radiative Forcing over Kanpur

Aerosol radiative forcing (ARF) at top of the atmosphere (ARF_{TOA}) and at the surface (ARF_{SRF}) is defined as the net difference in fluxes (both shortwave + longwave) between with and without aerosol at top of the atmosphere (TOA) and surface (SRF) respectively. In the present study, ARF is obtained at the TOA and SRF from AERONET which calculated the radiative forcing using a

radiative transfer model, GAME (Global Atmospheric ModEl). GAME is well accepted radiative model and performs spectral integration using correlated-k distribution based on line by line simulations (Scott, 1974). ARF at TOA, SRF and in the atmosphere (ATM) over Kanpur is shown in Figure 15 (a) and 15 (b) during the dust events occurred in May and June respectively. The ARF_{SRF} and ARF_{TOA} values are always negative for both the dust events and found in the rage of -101 to -191 Wm^{-2} and -12 to -37 Wm^{-2} in May while 90 to -151 Wm^{-2} and -47 to -64 Wm^{-2} in June respectively. A significant change in ARF is observed with higher magnitude of ARF (both ARF_{SRF} and ARF_{TOA}) during the both the dust storm days suggesting the more attenuation of surface reaching solar radiation, which may be mainly because of backscattering due to aerosol particles. However, the positive value of ARF in to the atmosphere (ARF_{ATM} = ~ 124 Wm^{-2} on 17 May, 2018 and ARM_{ATM} = ~ 85 Wm^{-2} on 14 June, 2018) suggest the net warming effect of the atmosphere due to the aerosol during the events. Recently, Kumar et al. (2015) calculated the ARF over Kanpur during the dust storms occurred in 2010 and found in the range of - 66 to -101 Wm^{-2}, -18 to -41 Wm^{-2} and + 37 to +75 Wm^{-2} for the ARF_{SRF}, ARF_{TOA}, and ARF_{ATM} respectively while Kaskaoutis et al. (2013) found relatively lower ARF value i. e. -69 to -97 Wm^{-2}, -20 to 30 Wm^{-2} and 43 to 71 Wm^{-2} for ARF_{SRF}, ARF_{TOA}, and ARF_{ATM} respectively. Similar range of ARF is also reported also reported over different station in IGB i.e. over Patiala (+45 to +77 Wm^{-2}) by Singh et al. (2016), over Delhi (+27 Wm^{-2} in March and +123 Wm^{-2} in June) by Pandithurai et al. (2008), over Gandhi College (~ +18 Wm^{-2}) by Srivastava et al. (2011) and also over Nainital (+38 Wm^{-2}) by Dumka et al. (2014). The atmospheric heating rate is also calculated by the equation given below:

$$\frac{\partial T}{\partial t} = \frac{g}{Cp} * \frac{\Delta F_{ATM}}{\Delta P} \qquad (2)$$

where $\partial T/\partial t$ is the heating rate (Kelvin day^{-1}), g is the acceleration due to gravity, C_p is the specific heat capacity of air at constant atmospheric pressure and ΔP is the pressure difference. Since most of the aerosols are confined close to the surface i.e. maximum up to 3 – 4 km during dust storm

events over IGB (Kedia et al., 2018; Kumar et al., 2015, 2014). Therefore, in the present study, ΔP is taken as 300 hPa. The atmospheric heating range is found in the range of 1.51 – 3.88 K day^{-1} and 0.9 – 1.88 K day^{-1} in May and June respectively which are given in Table 3. Higher value of atmospheric heating rate during dust storm days (17 May 2018, and 14 June 2018) due to the abundance of dust aerosol is quite significant to affect the atmospheric dynamics. Lau et al. (2006) found abnormal in atmospheric heating rate over Northern India during pre-monsoon season, mainly attributed to the enhancement in dust particle which leads to affect intensification of the Indian summer monsoon system. Similar range of atmospheric heating rate during dust storm is also reported by earlier researchers with value in the range of 0.7 to 1.4 K day^{-1} (Iftikhar et al., 2018) over Karachi, 1.3 – 2.2 K day^{-1} over Lahore (Iftikhar et al., 2018), 2.0 K day^{-1} over Jodhpur (Srivastava et al., 2014), 1.9 K day^{-1} over Delhi (Srivastava et al., 2014), 1.3 to 2.2 K day^{-1} over Patiala (Singh et al., 2016), 0.78 to 1.57 K day^{-1} over Kanpur (Kumar et al., 2015). Tiwari et al. (2015) also reported similar range of atmospheric heating for polluted dust aerosol over entire IGB. Further detailed studies on the impacts of enhanced aerosol heating during this severe dust storm and its effect on regional climate are highly needed.

5. Conclusion:

The present study is mainly focused to investigate the impact of the intense dust storm on aerosol characteristics and **radiative impacts** over northern India during the pre-monsoon season of 2018 using satellite observation in combination with ground observed (AERONET), model and reanalysis data. Although, significant impacts of dust storms were observed at Kanpur yet the main findings are summarized as:

- The MODIS true colour images, along with air mass back trajectory pathways and DREAM model simulated results identified the Thar Desert as the major source of dust storm which

enhances the aerosol burden over entire IGB region during the dust storm.

- A higher value of AOD and AI value is observed over entire IGB during the dust storms which is more prominence on 14th June 2018. The figures also further confirm the Thar Desert region as a major contributor of aerosol during the dust storm events. The spatial distribution of enhancement factor of AOD and AI suggest that dust storm on 17 May 2018 have relatively larger impacts on monthly mean AOD as well seasonal (pre-monsoon season) mean AOD than 14 June 2018 which may be due to the frequent occurrence of dust aerosol over northern India during June.

- Aerosol characteristics over Kanpur were studied by using AERONET data which show prominent alteration during the dust storm days. The AOD value increases up to nearly more than **two-fold** during dust storm days with minimum AE (440 – 870 nm) value nearly zero suggesting the abundance of coarse mode aerosol particles which is also supported aerosol volume size distribution. The higher value of SSA (>0.9 at 675 nm) is observed which show an increasing spectral trend with wavelength suggesting the dominance of scattering type of aerosols which is also confirmed by the spectral variability of asymmetry parameter and refractive indices (both real and imaginary). The enhancement in columnar water vapour after the dust storms suggests the transportation of moisture from the Arabian Sea through the dust storm.

- The CALIPSO observation suggesting the presence of an elevated aerosol layer over IGB during the two intense dust storm days which may be sufficient to affect Indian Summer Monsoon (ISM) by warming the lower and mid troposphere. Thus, the present study indicates towards the further investigation of the relation between the dust concentration, transportation and their impact on the Indian Summer Monsoon.

- The outgoing longwave radiation is found maximum over the Thar Desert region and IGB during the two intense dust storm days and resulting to enhancement in OLR on monthly and seasonally mean value in the range of 20 – 50 Wm^{-2}. However, the estimated radiative forcing over Kanpur

shows a significant cooling (-160 Wm^{-2} on 17 May 2018 and -141 Wm^{-2} on 14 June, 2018) at the surface and warming (+124 Wm^{-2} on 17 May 2018 and 85 Wm^{-2} on 14 June, 2018) in the atmosphere with large heating rate (2.69 $Kday^{-1}$ on 17 May 2018 and 1.85 $Kday^{-1}$ on 14 June, 2018) during the dust storm days which may be significant to affect atmospheric dynamics, monsoon circulation and hydrological cycle.

Acknowledgement:

We are thankful to MODIS, CALIPSO, OMI and AERONET NASA scientific research team for providing aerosol data. We acknowledge the use of National Centre for Environmental Prediction (NCEP) for synoptic meteorological data and NOAA HYSPLIT model for back trajectory analysis. One of the authors, Mr Akhilesh Kumar is also thankful to Department of Science and Technology, New Delhi for providing INSPIRE research fellowship. The use of BSC-DREAM8b model is dully acknowledged. The work is partly supported by ISRO, Bangalore under ISRO-SSPS programme and **DST, New Delhi under DST-FIST Program**. Author **Shani** Tiwari is also thankful to the Shandong University, China for the financial support under the International Postdoctoral Exchange Program.

Reference:

Ackerman, S.A. and Chung, H., 1992. Radiative effects of Airborne Dust on Regional Energy Budgets at the Top of the Atmosphere. J. Appl. Meteor. 31, 223–233. https://doi.org/10.1175/1520-0450(1992)

Aher, G.R., Pawar, G. V., Gupta, P., Devara, P.C.S., 2014. Effect of major dust storm on optical, physical, and radiative properties of aerosols over coastal and urban environments in Western India. International Journal of Remote Sensing 35, 871–903. https://doi.org/10.1080/01431161.2013.873153

Alam, K., Trautmann, T., Blaschke, T., 2011. Aerosol optical properties and radiative forcing over mega-city Karachi. Atmospheric Research 101, 2011-05. https://doi.org/10.1016/j.atmosres.2011.05.007

Alam, K., Trautmann, T., Blaschke, T., Majid, H., 2012. Aerosol optical and radiative properties during summer and winter seasons over Lahore and Karachi. Atmospheric Environment 50, 234-245. https://doi.org/10.1016/j.atmosenv.2011.12.027

Alam, K., Trautmann, T., Blaschke, T., Subhan, F., 2014. Changes in aerosol optical properties due to dust storms in the Middle East and Southwest Asia. Remote Sensing of Environment 143, 216–227. https://doi.org/10.1016/j.rse.2013.12.021

Altaratz, O., Koren, I., Remer, L.A., Hirsch, E., 2014. Review: Cloud invigoration by aerosols-Coupling between microphysics and dynamics. Atmospheric Research 140–141, 38–60. https://doi.org/10.1016/j.atmosres.2014.01.009

Amiridis, V., Balis, D.S., Giannakaki, E., Stohl, A., Kazadzis, S., Koukouli, M.E., Zanis, P., 2009. Optical characteristics of biomass burning aerosols over Southeastern Europe determined from UV-Raman lidar measurements. Atmospheric Chemistry and Physics 9, 2431-2440. https://doi.org/10.5194/acp-9-2431-2009

Ångström, A., 1964. The parameters of atmospheric turbidity. Tellus 16, 64–75. https://doi.org/10.1111/j.2153-3490.1964.tb00144.x

Badarinath, K.V.S., Kharol, S.K., Kaskaoutis, D.G., Sharma, A.R., Ramaswamy, V., Kambezidis, H.D., 2010. Long-range transport of dust aerosols over the Arabian Sea and Indian region - A case study using satellite data and ground-based measurements. Global and Planetary Change 72(3):164-181. https://doi.org/10.1016/j.gloplacha.2010.02.003

Bergstrom, R.W., Pilewskie, P., Russell, P.B., Redemann, J., Bond, T.C., Quinn, P.K., Sierau, B., 2007. Spectral absorption properties of atmospheric aerosols. Atmospheric Chemistry and Physics 7, 5937-5943. https://doi.org/10.5194/acp-7-5937-2007

Boucher, O., Randall, D., Artaxo, P., Bretherton, C.S., 2013. Chapter 7 : Clouds and Aerosols. Biomass 571-658. https://doi.org/10.1017/CBO9781107415324.016

Bran, S.H., Jose, S., Srivastava, R., 2018. Investigation of optical and radiative properties of aerosols during an intense dust storm: A regional climate modeling approach. Journal of Atmospheric and Solar-Terrestrial Physics 168. https://doi.org/10.1016/j.jastp.2018.01.003

Bucci, S., Cagnazzo, C., Cairo, F., Di Liberto, L., Fierli, F., 2014. Aerosol variability and atmospheric transport in the Himalayan region from CALIOP 2007-2010 observations. Atmospheric Chemistry and Physics 14, 4369-4381. https://doi.org/10.5194/acp-14-4369-2014

Carugno, M., Consonni, D., Randi, G., Catelan, D., Grisotto, L., Bertazzi, P.A., Biggeri, A., Baccini, M., 2016. Air pollution exposure, cause-specific deaths and hospitalizations in a highly polluted italian region. Environmental Research 147, 415-424. https://doi.org/10.1016/j.envres.2016.03.003

Crosbie, E., Sorooshian, A., Monfared, N.A., Shingler, T., Esmaili, O., 2014. A multi-year aerosol characterization for the greater tehran area using satellite, surface, and modeling data. Atmosphere *5*(2), 178-197. https://doi.org/10.3390/atmos5020178

Curier, R.L., Veefkind, J.P., Braak, R., Veihelmann, B., Torres, O., de Leeuw, G., 2008. Retrieval of aerosol optical properties from OMI radiances using a multiwavelength algorithm: Application to western Europe. Journal of Geophysical Research Atmospheres 113, D17S90. https://doi.org/10.1029/2007JD008738

Dey, S., Tripathi, S.N., Singh, R.P., Holben, B.N., 2004. Influence of dust storms on the aerosol optical properties over the Indo-Gangetic basin. Journal of Geophysical Research D: Atmospheres 109, D20211. https://doi.org/10.1029/2004JD004924

Draxler, R.R., Rolph, G.D., 2003. HYSPLIT (HYbrid Single-Particle Lagrangian Integrated Trajectory). NOAA Air Resources Laboratory, College Park, MD.

Du, M., Yonemura, S., Shen, Y., Wang, W., 2018. Changes of Long-wave and Sort-wave Radiations at Ground Surface during Dust Storms at Dunhuang, China, in: IOP Conference Series: Materials Science and Engineering 301, 012167. https://doi.org/10.1088/1757-899X/301/1/012167

Dubovik, O., Holben, B., Eck, T.F., Smirnov, A., Kaufman, Y.J., King, M.D., Tanré, D., Slutsker, I., 2002a. Variability of Absorption and Optical Properties of Key Aerosol Types Observed in Worldwide Locations. Journal of the Atmospheric Sciences 59, 590–608. https://doi.org/10.1175/1520-0469(2002)

Dubovik, O., Holben, B.N., Lapyonok, T., Sinyuk, A., Mishchenko, M.I., Yang, P., Slutsker, I., 2002b. Non-spherical aerosol retrieval method employing light scattering by spheroids. Geophysical Research Letters 29, 54-1-54–4. https://doi.org/10.1029/2001GL014506

Dubovik, O., Holben, B.N., Kaufman, Y.J., Yamasoe, M., Smimov, A., Tanré, D., Slutsker, I., 1998. Single-scattering albedo of smoke retrieved from the sky radiance and solar transmittance measured from ground. Journal of Geophysical Research Atmospheres 103, D24, 31903-31923. https://doi.org/10.1029/98JD02276

Dubovik, O., King, M.D., 2000. A flexible inversion algorithm for retrieval of aerosol optical properties from Sun and sky radiance measurements. Journal of Geophysical Research Atmospheres 105, 20673–20696. https://doi.org/10.1029/2000JD900282

Dubovik, O., Smirnov, A., Holben, B.N., King, M.D., Kaufman, Y.J., Eck, T.F., Slutsker, I., 2000. Accuracy assessments of aerosol optical properties retrieved from Aerosol Robotic Network (AERONET) Sun and sky radiance measurements. Journal of Geophysical Research Atmospheres 105, 9791–9806. https://doi.org/10.1029/2000JD900040

Dumka, U.C., Tripathi, S.N., Misra, A., Giles, D.M., Eck, T.F., Sagar, R., Holben, B.N., 2014. Latitudinal variation of aerosol properties from Indo-Gangetic Plain to central Himalayan foothills during TIGERZ campaign. Journal of Geophysical Research 119, 4750–4769. https://doi.org/10.1002/2013JD021040

Eck, T.F., Holben, B.N., Reid, J.S., Dubovik, O., Smirnov, A., O'Neill, N.T., Slutsker, I., Kinne, S., 1999. Wavelength dependence of the optical depth of biomass burning, urban, and desert dust aerosols. Journal of Geophysical Research 104, D24, 31333-31349. https://doi.org/10.1029/1999JD900923

Eck, T.F., Holben, B.N., Smirnov, A., Slutsker, I., Lobert, J.M., Ramanathan, V., 2001. Column-integrated aerosol optical properties over the Maidives during the northeast 106, 555–566.

El-Askary, H., 2015. On the Detection and Monitoring of the Transport of an Asian Dust Storm Using Multi-Sensor Satellite Remote Sensing. Journal of Environmental Informatics 25, 99–116. https://doi.org/10.3808/jei.201500306

El-Askary, H., Gautam, R., Singh, R.P., Kafatos, M., 2006. Dust storms detection over the Indo-Gangetic basin using multi sensor data. Advances in Space Research 37, 728–733. https://doi.org/10.1016/j.asr.2005.03.134

Filonchyk, M., Yan, H., Shareef, T.M.E., Yang, S., 2018. Aerosol contamination survey during dust storm process in Northwestern China using ground, satellite observations and atmospheric modeling data. Theoretical and Applied Climatology 1–15. https://doi.org/10.1007/s00704-017-2362-8

Gautam, R., Hsu, N.C., Eck, T.F., Holben, B.N., Janjai, S., Jantarach, T., Tsay, S.C., Lau, W.K., 2013. Characterization of aerosols over the Indochina peninsula from satellite-surface observations during biomass burning pre-monsoon season. Atmospheric Environment 78, 51–59. https://doi.org/10.1016/j.atmosenv.2012.05.038

Gautam, R., Hsu, N.C., Lau, K.M., 2010. Premonsoon aerosol characterization and radiative effects over the Indo-Gangetic plains: Implications for regional climate warming. Journal of Geophysical Research Atmospheres 115 (D17). https://doi.org/10.1029/2010JD013819

Gautam, R., Hsu, N.C., Lau, K.M., Tsay, S.C., Kafatos, M., 2009. Enhanced pre-monsoon warming over the Himalayan-Gangetic region from 1979 to 2007. Geophysical Research Letters 36, 1–5. https://doi.org/10.1029/2009GL037641

Gautam, R., Hsu, N.C., Tsay, S.C., Lau, K.M., Holben, B., Bell, S., Smirnov, A., Li, C., Hansell, R., Ji, Q., Payra, S., Aryal, D., Kayastha, R., Kim, K.M., 2011. Accumulation of aerosols over the Indo-Gangetic plains and southern slopes of the Himalayas: Distribution, properties and radiative effects during the 2009 pre-monsoon season. Atmospheric Chemistry and Physics 11,

12841–12863. https://doi.org/10.5194/acp-11-12841-2011

Gharai, B., Jose, S., Mahalakshmi, D. V, 2013. Monitoring intense dust storms over the Indian region using satellite data - a case study. International Journal of Remote Sensing 34, 7038–7048. https://doi.org/10.1080/01431161.2013.813655

Ginoux, P., Prospero, J.M., Gill, T.E., Hsu, N.C., Zhao, M., 2012. Global-scale attribution of anthropogenic and natural dust sources and their emission rates based on MODIS Deep Blue aerosol products. Reviews of Geophysics 50 RG3005. https://doi.org/10.1029/2012RG000388

Gobbi, G.P., Barnaba, F., Giorgi, R., Santacasa, A., 2000. Altitude-resolved properties of a Saharan dust event over the Mediterranean. Atmospheric Environment 34(29):5119-5127. https://doi.org/10.1016/S1352-2310(00)00194-1

Guo, J., Yin, Y., 2015. Mineral dust impacts on regional precipitation and summer circulation in East Asia using a regional coupled climate system model. Journal of Geophysical Research 120, 10378-10398. https://doi.org/10.1002/2015JD023096

Hamonou, E., Chazette, P., Balis, D., Dulac, F., Schneider, X., Galani, E., Ancellet, G., Papayannis, A., 1999. Characterization of the vertical structure of Saharan dust export to the Mediterranean basin. Journal of Geophysical Research Atmospheres 104, 22257–22270. https://doi.org/10.1029/1999JD900257

Hansell, R.A., Tsay, S.C., Ji, Q., Hsu, N.C., Jeong, M.J., Wang, S.H., Reid, J.S., Liou, K.N., Ou, S.C., 2010. An Assessment of the Surface Longwave Direct Radiative Effect of Airborne Saharan Dust during the NAMMA Field Campaign. Journal of the Atmospheric Sciences 67, 1048–1065. https://doi.org/10.1175/2009JAS3257.1

Haustein, K., Pérez, C., Baldasano, J.M., Müller, D., Tesche, M., Schladitz, A., Esselborn, M., Weinzierl, B., Kandler, K., Von Hoyningen-Huene, W., 2009. Regional dust model performance during SAMUM 2006. Geophysical Research Letters 36, L03812. https://doi.org/10.1029/2008GL036463

Haywood, J.M., Allan, R.P., Culverwell, I., Slingo, T., Milton, S., Edwards, J., Clerbaux, N., 2005. Can desert dust explain the outgoing longwave radiation anomaly over the Sahara during July 2003? Journal of Geophysical Research D: Atmospheres 110, D05105. https://doi.org/10.1029/2004JD005232

Holben, B.N., Eck, T.F., Slutsker, I., Tanré, D., Buis, J.P., Setzer, A., Vermote, E., Reagan, J.A., Kaufman, Y.J., Nakajima, T., Lavenu, F., Jankowiak, I., Smirnov, A., 1998. AERONET—A Federated Instrument Network and Data Archive for Aerosol Characterization. Remote Sensing of Environment 66, 1–16. https://doi.org/10.1016/S0034-4257(98)00031-5

Hsu, N.C., Herman, J.R., Torres, O., Holben, B.N., Tanre, D., Eck, T.F., Smirnov, A., Chatenet, B.,

Lavenu, F., 1999. Comparisons of the TOMS aerosol index with Sun-photometer aerosol optical thickness: Results and applications. Journal of Geophysical Research Atmospheres 104, D6, 6269-6279. https://doi.org/10.1029/1998JD200086

Hsu, N.C., Herman, J.R., Weaver, C., 2000. Determination of radiative forcing of Saharan dust using combined TOMS and ERBE data. Journal of Geophysical Research 105, D16, 20649-20661. https://doi.org/10.1029/2000JD900150

Hsu, N.C., Tsay, S.C., King, M.D., Herman, J.R., 2006. Deep Blue retrievals of Asian aerosol properties during ACE-Asia. IEEE Transactions on Geoscience and Remote Sensing 44, 3180 - 3195. https://doi.org/10.1109/TGRS.2006.879540

Huneeus, N., Schulz, M., Balkanski, Y., Griesfeller, J., Prospero, J., Kinne, S., Bauer, S., Boucher, O., Chin, M., Dentener, F., Diehl, T., Easter, R., Fillmore, D., Ghan, S., Ginoux, P., Grini, A., Horowitz, L., Koch, D., Krol, M.C., Landing, W., Liu, X., Mahowald, N., Miller, R., Morcrette, J.J., Myhre, G., Penner, J., Perlwitz, J., Stier, P., Takemura, T., Zender, C.S., 2011. Global dust model intercomparison in AeroCom phase i. Atmospheric Chemistry and Physics 11, 7781-7816. https://doi.org/10.5194/acp-11-7781-2011

Iftikhar, M., Alam, K., Sorooshian, A., Syed, W.A., Bibi, S., Bibi, H., 2018. Contrasting aerosol optical and radiative properties between dust and urban haze episodes in megacities of Pakistan. Atmospheric Environment 173, 157-172. https://doi.org/10.1016/j.atmosenv.2017.11.011

IPCC, 2013. IPCC Fifth Assessment Report, Climatic Change 2013: The Physical Science Basis. the Intergovernmental Panel on Climate Change. https://doi.org/10.1017/CBO9781107415324

Jin, Q., Wei, J., Yang, Z.L., 2014. Positive response of Indian summer rainfall to Middle East dust. Geophysical Research Letters 41, 4068-4074. https://doi.org/10.1002/2014GL059980

Kaskaoutis, D.G., Gautam, R., Singh, R.P., Houssos, E.E., Goto, D., Singh, S., Bartzokas, A., Kosmopoulos, P.G., Sharma, M., Hsu, N.C., Holben, B.N., Takemura, T., 2012. Influence of anomalous dry conditions on aerosols over India: Transport, distribution and properties. Journal of Geophysical Research Atmospheres 117, D09106. https://doi.org/10.1029/2011JD017314

Kaskaoutis, D.G., Houssos, E.E., Goto, D., Bartzokas, A., Nastos, P.T., Sinha, P.R., Kharol, S.K., Kosmopoulos, P.G., Singh, R.P., Takemura, T., 2014. Synoptic weather conditions and aerosol episodes over Indo-Gangetic Plains, India. Climate Dynamics 43, 2313–2331. https://doi.org/10.1007/s00382-014-2055-2

Kaskaoutis, D.G., Houssos, E.E., Solmon, F., Legrand, M., Rashki, A., Dumka, U.C., Francois, P., Gautam, R., Singh, R.P., 2018. Impact of atmospheric circulation types on southwest Asian dust and Indian summer monsoon rainfall. Atmospheric Research 201, 189-205. https://doi.org/10.1016/j.atmosres.2017.11.002

Kaskaoutis, D.G., Kalapureddy, M.C.R., Krishna Moorthy, K., Devara, P.C.S., Nastos, P.T., Kosmopoulos, P.G., Kambezidis, H.D., 2010. Heterogeneity in pre-monsoon aerosol types over the Arabian Sea deduced from ship-borne measurements of spectral AODs. Atmospheric Chemistry and Physics 10, 4893–4908. https://doi.org/10.5194/acp-10-4893-2010

Kaskaoutis, D.G., Kambezidis, H.D., Dumka, U.C., Psiloglou, B.E., 2016. Dependence of the spectral diffuse-direct irradiance ratio on aerosol spectral distribution and single scattering albedo. Atmospheric Research 178, 84-94. https://doi.org/10.1016/j.atmosres.2016.03.018

Kaskaoutis, D.G., Kambezidis, H.D., Hatzianastassiou, N., Kosmopoulos, P.G., Badarinath, K.V.S., 2007. Aerosol climatology: dependence of the Angstrom exponent on wavelength over four AERONET sites. Atmospheric Chemistry and Physics Discussions 7, 7347–7397. https://doi.org/10.5194/acpd-7-7347-2007

Kaskaoutis, D.G., Kambezidis, H.D., Nastos, P.T., Kosmopoulos, P.G., 2008. Study on an intense dust storm over Greece. Atmospheric Environment 42(29), 6884-6896. https://doi.org/10.1016/j.atmosenv.2008.05.017

Kaskaoutis, D.G., Sinha, P.R., Vinoj, V., Kosmopoulos, P.G., Tripathi, S.N., Misra, A., Sharma, M., Singh, R.P., 2013. Aerosol properties and radiative forcing over Kanpur during severe aerosol loading conditions. Atmospheric Environment 79, 7-19. https://doi.org/10.1016/j.atmosenv.2013.06.020

Kaufman, Y.J., Tanré, D., 1998. Algorithm for remote sensing of tropospheric aerosol from MODIS. MODIS ATBD: Remote Sensing of aerosol. http://modis-atmos.gsfc.nasa.gov/_docs/atbd_mod02.pdf. Accessed 26 Oct 1998

Kaufman, Y.J., Tanré, D., Remer, L.A., Vermote, E.F., Chu, A., Holben, B.N., 1997. Operational remote sensing of tropospheric aerosol over land from EOS moderate resolution imaging spectroradiometer. Journal of Geophysical Research: Atmospheres 102, D14, 17051-17067. https://doi.org/10.1029/96JD03988

Kedia, S., Kumar, R., Islam, S., Sathe, Y., Kaginalkar, A., 2018. Radiative impact of a heavy dust storm over India and surrounding oceanic regions. Atmospheric Environment 185, 109-120. https://doi.org/10.1016/j.atmosenv.2018.05.005

Kim, D., Chin, M., Yu, H., Eck, T.F., Sinyuk, A., Smirnov, A., Holben, B.N., 2011. Dust optical properties over North Africa and Arabian Peninsula derived from the AERONET dataset. Atmospheric Chemistry and Physics 11, 10733–10741. https://doi.org/10.5194/acp-11-10733-2011

Kim, S.W., Yoon, S.C., Jefferson, A., Won, J.G., Dutton, E.G., Ogren, J.A., Anderson, T.L., 2004.

Observation of enhanced water vapor in Asian dust layer and its effect on atmospheric radiative heating rates. Geophysical Research Letters 31, L18113. https://doi.org/10.1029/2004GL020024

King, M.D., Kaufman, Y.J., Menzel, W.P., Tanre, D., 1992. Remote Sensing of Cloud, Aerosol, and Water Vapor Properties from the Moderate Resolution Imaging Spectrometer (MODIS). IEEE Transactions on Geoscience and Remote Sensing 30, 2–27. https://doi.org/10.1109/36.124212

King, M.D., Menzel, W.P., Kaufman, Y.J., Tanre, D., Bo-Cai Gao, Platnick, S., Ackerman, S.A., Remer, L.A., Pincus, R., Hubanks, P.A., 2003. Cloud and aerosol properties, precipitable water, and profiles of temperature and water vapor from MODIS. IEEE Transactions on Geoscience and Remote Sensing 41, 442–458. https://doi.org/10.1109/TGRS.2002.808226

Kinne, S., Schulz, M., Textor, C., Guibert, S., Balkanski, Y., Bauer, S.E., Berntsen, T., Berglen, T.F., Boucher, O., Chin, M., Collins, W., Dentener, F., Diehl, T., Easter, R., Feichter, J., Fillmore, D., Ghan, S., Ginoux, P., Gong, S., Grini, A., Hendricks, J., Herzog, M., Horowitz, L., Isaksen, I., Iversen, T., Kirkevåg, A., Kloster, S., Koch, D., Kristjansson, J.E., Krol, M., Lauer, A., Lamarque, J.F., Lesins, G., Liu, X., Lohmann, U., Montanaro, V., Myhre, G., Penner, J.E., Pitari, G., Reddy, S., Seland, O., Stier, P., Takemura, T., Tie, X., 2006. An AeroCom initial assessment - Optical properties in aerosol component modules of global models. Atmospheric Chemistry and Physics 5(5):8285-8330. https://doi.org/10.5194/acp-6-1815-2006

Koepke, P., Hess, M., Schult, I., Shettle, E.P., 1997. Global Aerosol Data Set, Max-Planck-Institut fur Meteorologie. https://doi.org/ISSN: 0937-1060

Kubilay, N., Cokacar, T., Oguz, T., 2003. Optical properties of mineral dust outbreaks over the northeastern Mediterranean. Journal of Geophysical Research: Atmospheres 108, D21, 4666. https://doi.org/10.1029/2003JD003798

Kumar, R., Barth, M.C., Pfister, G.G., Naja, M., Brasseur, G.P., 2014. WRF-Chem simulations of a typical pre-monsoon dust storm in northern India: Influences on aerosol optical properties and radiation budget. Atmospheric Chemistry and Physics 14, 2431-244. https://doi.org/10.5194/acp-14-2431-2014

Kumar, S., Kumar, S., Kaskaoutis, D.G., Singh, R.P., Singh, R.K., Mishra, A.K., Srivastava, M.K., Singh, A.K., 2015. Meteorological, atmospheric and climatic perturbations during major dust storms over Indo-Gangetic Basin. Aeolian Research 17, 15–31. https://doi.org/10.1016/j.aeolia.2015.01.006

Kumar, S., Singh, A., Prasad, A., 2009. Annual variability of water vapor from GPS and MODIS data over the Indo-Gangetic Plains 13, 17-23. J. Ind. Geophys. Union.

Labonne, M., Bréon, F.M., Chevallier, F., 2007. Injection height of biomass burning aerosols as seen

from a spaceborne lidar. Geophysical Research Letters 34: L11806. https://doi.org/10.1029/2007GL029311

Lafon, S., Sokolik, I.N., Rajot, J.L., Caquincau, S., Gaudichet, A., 2006. Characterization of iron oxides in mineral dust aerosols: Implications for light absorption. Journal of Geophysical Research Atmospheres 111, D21207. https://doi.org/10.1029/2005JD007016

Lau, K.M., Kim, M.K., Kim, K.M., 2006. Asian summer monsoon anomalies induced by aerosol direct forcing: The role of the Tibetan Plateau. Climate Dynamics 86, 855–864. https://doi.org/10.1007/s00382-006-0114-z

Lemaître, C., Flamant, C., Cuesta, J., Raut, J.C., Chazette, P., Formenti, P., Pelon, J., 2010. Radiative heating rates profiles associated with a springtime case of Bodélé and Sudan dust transport over West Africa. Atmospheric Chemistry and Physics 10, 8131-8150. https://doi.org/10.5194/acp-10-8131-2010

Léon, J.F., Legrand, M., 2003. Mineral dust sources in the surroundings of the North Indian Ocean. Geophysical Research Letters 30(6):1309. https://doi.org/10.1029/2002GL016690

Levelt, P.F., Van Den Oord, G.H.J., Dobber, M.R., Mälkki, A., Visser, H., De Vries, J., Stammes, P., Lundell, J.O. V, Saari, H., 2006. The ozone monitoring instrument. IEEE Transactions on Geoscience and Remote Sensing 44, 1093 - 1101. https://doi.org/10.1109/TGRS.2006.872333

Levy, R.C., Remer, L.A., Kleidman, R.G., Mattoo, S., Ichoku, C., Kahn, R., Eck, T.F., 2010. Global evaluation of the Collection 5 MODIS dark-target aerosol products over land. Atmospheric Chemistry and Physics 10, 10399-10420. https://doi.org/10.5194/acp-10-10399-2010

Levy, R.C., Remer, L.A., Mattoo, S., Vermote, E.F., Kaufman, Y.J., 2007. Second-generation operational algorithm: Retrieval of aerosol properties over land from inversion of Moderate Resolution Imaging Spectroradiometer spectral reflectance. Journal of Geophysical Research Atmospheres 112, D13211. https://doi.org/10.1029/2006JD007811

Liu, D., Abuduwaili, J., Lei, J., Wu, G., Gui, D., 2011. Wind erosion of saline playa sediments and its ecological effects in Ebinur Lake, Xinjiang, China. Environmental Earth Sciences 63(2):241–250. https://doi.org/10.1007/s12665-010-0690-4

Liu, D., Wang, Y., Wang, Z., Zhou, J., 2012. The three-dimensional structure of transatlantic african dust transport: A new perspective from CALIPSO LIDAR measurements. Advances in Meteorology 2012, ID850704. https://doi.org/10.1155/2012/850704

Mahowald, N., 2011. Aerosol indirect effect on biogeochemical cycles and climate. Science 334(6057): 794-796. https://doi.org/10.1126/science.1207374

Mandija, F., Sicard, M., Comerón, A., Alados-Arboledas, L., Guerrero-Rascado, J.L., Bravo-Aranda, J.A., Bravo-Aranda, J.A., Granados-Muñoz, M.J., Lyamani, H., Muñoz Porcar, C.,

Rocadenbosch, F., Rodríguez, A., Valenzuela, A., García Vizcaíno, D., 2017. Origin and pathways of the mineral dust transport to two Spanish EARLINET sites: Effect on the observed columnar and range-resolved dust optical properties. Atmospheric Research 187, 69-83. https://doi.org/10.1016/j.atmosres.2016.12.002

Mishra, A.K., Shibata, T., 2012. Synergistic analyses of optical and microphysical properties of agricultural crop residue burning aerosols over the Indo-Gangetic Basin (IGB). Atmospheric Environment 172, 83-92. https://doi.org/10.1016/j.atmosenv.2012.04.025

Namdari, S., Karimi, N., Sorooshian, A., Mohammadi, G.H., Sehatkashani, S., 2018. Impacts of climate and synoptic fluctuations on dust storm activity over the Middle East. Atmospheric Environment 173, 265-276. https://doi.org/10.1016/j.atmosenv.2017.11.016

Nastos, P.T., 2012. Meteorological patterns associated with intense saharan dust outbreaks over greece in winter. Advances in Meteorology 2012. https://doi.org/10.1155/2012/828301

Nickovic, S., Kallos, G., Papadopoulos, A., Kakaliagou, O., 2001. A model for prediction of desert dust cycle in the atmosphere. Journal of Geophysical Research Atmospheres 106, D16, 18113-18129. https://doi.org/10.1029/2000JD900794

Obregón, M.A., Pereira, S., Salgueiro, V., Costa, M.J., Silva, A.M., Serrano, A., Bortoli, D., 2015. Aerosol radiative effects during two desert dust events in August 2012 over the southwestern Iberian Peninsula. Atmospheric Research 153, 404-415. https://doi.org/10.1016/j.atmosres.2014.10.007

Pandithurai, G., Seethala, C., Murthy, B.S., Devara, P.C.S., 2008. Investigation of atmospheric boundary layer characteristics for different aerosol absorptions: Case studies using CAPS model. Atmospheric Environment 42, 4755–4768. https://doi.org/10.1016/j.atmosenv.2008.01.038

Pant, P., Hegde, P., Dumka, U.C., Sagar, R., Satheesh, S.K., Moorthy, K.K., Saha, A., Srivastava, M.K., 2006. Aerosol characteristics at a high-altitude location in central Himalayas: Optical properties and radiative forcing. Journal of Geophysical Research Atmospheres 111. https://doi.org/10.1029/2005JD006768

Pérez, C., Nickovic, S., Baldasano, J.M., Sicard, M., Rocadenbosch, F., Cachorro, V.E., 2006. A long Saharan dust event over the western Mediterranean: Lidar, Sun photometer observations, and regional dust modeling. Journal of Geophysical Research Atmospheres 111. https://doi.org/10.1029/2005JD006579

Piedehierro, A.A., Antón, M., Cazorla, A., Alados-Arboledas, L., Olmo, F.J., 2014. Evaluation of enhancement events of total solar irradiance during cloudy conditions at Granada (Southeastern Spain). Atmospheric Research 135-136:1-7. https://doi.org/10.1016/j.atmosres.2013.08.008

Prasad, A.K., Singh, R.P., 2009. Validation of MODIS Terra, AIRS, NCEP/DOE AMIP-II Reanalysis-2, and AERONET Sun photometer derived integrated precipitable water vapor using ground-based GPS receivers over India. Journal of Geophysical Research Atmospheres 114, 1–20. https://doi.org/10.1029/2008JD011230

Prasad, A.K., Singh, R.P., 2007a. Changes in aerosol parameters during major dust storm events (2001-2005) over the Indo-Gangetic Plains using AERONET and MODIS data. Journal of Geophysical Research Atmospheres 112. https://doi.org/10.1029/2006JD007778

Prasad, A.K., Singh, R.P., Singh, A., 2006. Seasonal climatology of aerosol optical depth over the Indian subcontinent: Trend and departures in recent years. International Journal of Remote Sensing 27, 2323–2329. https://doi.org/10.1080/01431160500043665

Prasad, A.K., Singh, S., Chauhan, S.S., Srivastava, M.K., Singh, R.P., Singh, R., 2007b. Aerosol radiative forcing over the Indo-Gangetic plains during major dust storms. Atmospheric Environment 41, 6289–6301. https://doi.org/10.1016/j.atmosenv.2007.03.060

Pratap, V., Kumar, A., Singh, A.K., 2017. Short Term Air Quality Degradation by Firecrackers Used during Diwali Festival in Varanasi , India 18158–18165. https://doi.org/10.15680/IJIRSET.2017.0609079

Prijith, S.S., Rajeev, K., Thampi, B. V., Nair, S.K., Mohan, M., 2013. Multi-year observations of the spatial and vertical distribution of aerosols and the genesis of abnormal variations in aerosol loading over the Arabian Sea during Asian summer monsoon season. Journal of Atmospheric and Solar-Terrestrial Physics 105, 142-151. https://doi.org/10.1016/j.jastp.2013.09.009

Proestakis, E., Amiridis, V., Marinou, E., Georgoulias, A.K., Solomos, S., Kazadzis, S., Chimot, J., Che, H., Alexandri, G., Binietoglou, I., Daskalopoulou, V., Kourtidis, K.A., De Leeuw, G., Van Der A, R.J., 2018. Nine-year spatial and temporal evolution of desert dust aerosols over South and East Asia as revealed by CALIOP. Atmospheric Chemistry and Physics 18, 1337-1362. https://doi.org/10.5194/acp-18-1337-2018

Prospero, J.M., Ginoux, P., Torres, O., Nicholson, S.E., Gill, T.E., 2002. Environmental characterization of global sources of atmospheric soil dust identified with the Nimbus 7 Total Ozone Mapping Spectrometer (TOMS) absorbing aerosol product. Reviews of Geophysics 40(1), 2-1-2-31. https://doi.org/10.1029/2000RG000095

Prospero, J.M., Landing, W.M., Schulz, M., 2010. African dust deposition to Florida: Temporal and spatial variability and comparisons to models. Journal of Geophysical Research Atmospheres 115. https://doi.org/10.1029/2009JD012773

Ramachandran, S., Kedia, S., 2012. Radiative effects of aerosols over Indo-Gangetic plain: Environmental (urban vs. rural) and seasonal variations. Environmental Science and Pollution

Research 19(6): 2159–2171. https://doi.org/10.1007/s11356-011-0715-x

Ramachandran, S., Rajesh, T.A., 2008. Asymmetry parameters in the lower troposphere derived from aircraft measurements of aerosol scattering coefficients over tropical India. Journal of Geophysical Research Atmospheres 113. https://doi.org/10.1029/2008JD009795

Ramana, M. V., Ramanathan, V., Podgorny, I.A., Pradhan, B.B., Shrestha, B., 2004. The direct observations of large aerosol radiative forcing in the Himalayan region. Geophysical Research Letters 31. https://doi.org/10.1029/2003GL018824

Ramanathan, V., Chung, C., Kim, D., Bettge, T., Buja, L., Kiehl, J.T., Washington, W.M., Fu, Q., Sikka, D.R., Wild, M., 2005. Atmospheric brown clouds: Impacts on South Asian climate and hydrological cycle. Proceedings of the National Academy of Sciences 102, 5326–5333. https://doi.org/10.1073/pnas.0500656102

Ramaswamy, V., 2002. Infrared radiation in encyclopedia of global environmental change I, 470–475. Wiley, Hoboken

Raspanti, G.A., Hashibe, M., Siwakoti, B., Wei, M., Thakur, B.K., Pun, C.B., Al-Temimi, M., Lee, Y.C.A., Sapkota, A., 2016. Household air pollution and lung cancer risk among never-smokers in Nepal. Environmental Research 147, 141-145. https://doi.org/10.1016/j.envres.2016.02.008

Remer, L.A., Kaufman, Y.J., Tanré, D., Mattoo, S., Chu, D.A., Martins, J. V., Li, R.-R., Ichoku, C., Levy, R.C., Kleidman, R.G., Eck, T.F., Vermote, E., Holben, B.N., 2005. The MODIS Aerosol Algorithm, Products, and Validation. Journal of the Atmospheric Sciences 62, 947–973. https://doi.org/10.1175/JAS3385.1

Satheesh, S.K., Srinivasan, J., Moorthy, K.K., 2006. Spatial and temporal heterogeneity in aerosol properties and radiative forcing over Bay of Bengal: Sources and role of aerosol transport. Journal of Geophysical Research Atmospheres 111. https://doi.org/10.1029/2005JD006374

Scott, N.A., 1974. A direct method of computation of the transmission function of an inhomogeneous gaseous medium- I: Description of the method. Journal of Quantitative Spectroscopy and Radiative Transfer 14(8):691-704. https://doi.org/10.1016/0022-4073(74)90116-2

Seinfeld, J.H., Bretherton, C., Carslaw, K.S., Coe, H., DeMott, P.J., Dunlea, E.J., Feingold, G., Ghan, S., Guenther, A.B., Kahn, R., Kraucunas, I., Kreidenweis, S.M., Molina, M.J., Nenes, A., Penner, J.E., Prather, K.A., Ramanathan, V., Ramaswamy, V., Rasch, P.J., Ravishankara, A.R., Rosenfeld, D., Stephens, G., Wood, R., 2016. Improving our fundamental understanding of the role of aerosol−cloud interactions in the climate system. Proceedings of the National Academy of Sciences 113(21):5781-5790. https://doi.org/10.1073/pnas.1514043113

Sharma, D., Miller, R.L., 2017. Revisiting the observed correlation between weekly averaged Indian

monsoon precipitation and Arabian Sea aerosol optical depth. Geophysical Research Letters 44, 10006-10016. https://doi.org/10.1002/2017GL074373

Sharma, D., Singh, D., Kaskaoutis, D.G., 2012. Impact of two intense dust storms on aerosol characteristics and radiative forcing over Patiala, Northwestern India. Advances in Meteorology 2012. https://doi.org/10.1155/2012/956814

Shettle, E.P., Fenn, R.W., 1979. Models for the Aerosols of the Lower Atmosphere and the Effects of Humidity Variations on Their Optical Properties, Environmental Research Papers. https://doi.org/10.1109/TR.1987.5222381

Singh, A., Dey, S., 2012. Influence of aerosol composition on visibility in megacity Delhi. Atmospheric Environment 62, 367–373. https://doi.org/10.1016/j.atmosenv.2012.08.048

Singh, A., Tiwari, S., Sharma, D., Singh, D., Tiwari, S., Srivastava, A.K., Rastogi, N., Singh, A.K., 2016. Characterization and radiative impact of dust aerosols over northwestern part of India: a case study during a severe dust storm. Meteorology and Atmospheric Physics 128, 779–792. https://doi.org/10.1007/s00703-016-0445-1

Singh, S., Naseema Beegum, S., 2013. Direct radiative effects of an unseasonal dust storm at a western Indo Gangetic Plain station Delhi in ultraviolet, shortwave, and longwave regions. Geophysical Research Letters 40, 2444–2449. https://doi.org/10.1002/grl.50496

Singh, S., Nath, S., Kohli, R., Singh, R., 2005. Aerosols over Delhi during pre-monsoon months: Characteristics and effects on surface radiation forcing. Geophysical Research Letters 32, 1–4. https://doi.org/10.1029/2005GL023062

Sinyuk, A., Torres, O., Dubovik, O., 2003. Combined use of satellite and surface observations to infer the imaginary part of refractive index of Saharan dust. Geophysical Research Letters 30. https://doi.org/10.1029/2002GL016189

Slingo, A., Ackerman, T.P., Allan, R.P., Kassianov, E.I., McFarlane, S.A., Robinson, G.J., Barnard, J.C., Miller, M.A., Harries, J.E., Russell, J.E., Dewitte, S., 2006. Observations of the impact of a major Saharan dust storm on the atmospheric radiation balance. Geophysical Research Letters 33. https://doi.org/10.1029/2006GL027869

Sokolik, I.N., Toon, O.B., 1999. Incorporation of mineralogical composition into models of the radiative properties of mineral aerosol from UV to IR wavelengths. Journal of Geophysical Research Atmospheres 104, 9423–9444. https://doi.org/10.1029/1998JD200048

Solmon, F., Nair, V.S., Mallet, M., 2015. Increasing Arabian dust activity and the Indian summer monsoon. Atmospheric Chemistry and Physics 15, 8051-8064. https://doi.org/10.5194/acp-15-8051-2015

Solomon, S., Rosenlof, K.H., Portmann, R.W., Daniel, J.S., Davis, S.M., Sanford, T.J., Plattner,

G.K., 2010. Contributions of stratospheric water vapor to decadal changes in the rate of global warming. Science 327, 1219–1223. https://doi.org/10.1126/science.1182488

Sreekanth, V., Kulkarni, P., 2013. Spatio-temporal variations in columnar aerosol optical properties over Bay of Bengal: Signatures of elevated dust. Atmospheric Environment 69, 249-257. https://doi.org/10.1016/j.atmosenv.2012.12.031

Srivastava, A.K., Pant, P., Hegde, P., Singh, S., Dumka, U.C., Naja, M., Singh, N., Bhavanikumar, Y., 2011. The influence of a south asian dust storm on aerosol radiative forcing at a high-altitude station in central Himalayas. International Journal of Remote Sensing 32, 7827–7845. https://doi.org/10.1080/01431161.2010.531781

Srivastava, A.K., Singh, S., Tiwari, S., Bisht, D.S., 2012. Contribution of anthropogenic aerosols in direct radiative forcing and atmospheric heating rate over Delhi in the Indo-Gangetic Basin. Environmental Science and Pollution Research 19 (4), 1144-1158. https://doi.org/10.1007/s11356-011-0633-y

Srivastava, A.K., Soni, V.K., Singh, S., Kanawade, V.P., Singh, N., Tiwari, S., Attri, S.D., 2014. An early South Asian dust storm during March 2012 and its impacts on Indian Himalayan foothills: A case study. Science of the Total Environment 493, 526-534. https://doi.org/10.1016/j.scitotenv.2014.06.024

Srivastava, R., Ramachandran, S., 2013. The mixing state of aerosols over the Indo-Gangetic Plain and its impact on radiative forcing. Quarterly Journal of the Royal Meteorological Society 139, 137 – 151. https://doi.org/10.1002/qj.1958

Sun, Y., Clemens, S.C., Morrill, C., Lin, X., Wang, X., An, Z., 2012. Influence of Atlantic meridional overturning circulation on the East Asian winter monsoon. Nature Geoscience 5, 46–49. https://doi.org/10.1038/ngeo1326

Susskind, J., Molnar, G., Iredell, L., Loeb, N.G., 2012. Interannual variability of outgoing longwave radiation as observed by AIRS and CERES. Journal of Geophysical Research Atmospheres 117, D23107. https://doi.org/10.1029/2012JD017997

Tan, S.C., Li, J., Che, H., Chen, B., Wang, H., 2017. Transport of East Asian dust storms to the marginal seas of China and the southern North Pacific in spring 2010. Atmospheric Environment 148, 316-328. https://doi.org/10.1016/j.atmosenv.2016.10.054

Tanré, D., Herman, M., Kaufman, Y.J., 1996. Information on aerosol size distribution contained in solar reflected spectral radiances. Journal of Geophysical Research: Atmospheres 101, 19043–19060. https://doi.org/10.1029/96JD00333

Tiwari, S., Mishra A., Singh A. K., 2016a. Aerosol Climatology over the Bay of Bengal and Arabian Sea Inferred from Space-Borne Radiometers and Lidar Observations. Aerosol

and Air Quality Research, 16: 2855–2868

Tiwari, S., Kaskaoutis, D., Soni, V.K., Dev Attri, S., Singh, A.K., 2018. Aerosol columnar characteristics and their heterogeneous nature over Varanasi, in the central Ganges valley. Environmental Science and Pollution Research 25(25): 24726–24745. https://doi.org/10.1007/s11356-018-2502-4

Tiwari, S., Srivastava, A.K., Singh, A.K., 2013. Heterogeneity in pre-monsoon aerosol characteristics over the Indo-Gangetic Basin. Atmospheric Environment 77, 738-747. https://doi.org/10.1016/j.atmosenv.2013.05.035

Tiwari, S., Srivastava, A.K., Singh, A.K., Singh, S., 2015. Identification of aerosol types over Indo-Gangetic Basin : implications to optical properties and associated radiative forcing. Environmental Science and Pollution Research 12246–12260. https://doi.org/10.1007/s11356-015-4495-6

Tiwari, S., Tiwari, S., Hopke, P.K., Attri, S.D., Soni, V.K., Singh, A.K., 2016b. Variability in optical properties of atmospheric aerosols and their frequency distribution over a mega city "New Delhi," India. Environmental Science and Pollution Research. https://doi.org/10.1007/s11356-016-6060-3

Todd, M.C., Bou Karam, D., Cavazos, C., Bouet, C., Heinold, B., Baldasano, J.M., Cautenet, G., Koren, I., Perez, C., Solmon, F., Tegen, I., Tulet, P., Washington, R., Zakey, A., 2008. Quantifying uncertainty in estimates of mineral dust flux: An intercomparison of model performance over the Bodélé depression, northern Chad. Journal of Geophysical Research Atmospheres 113, D24107. https://doi.org/10.1029/2008JD010476

Torres, O., Ahn, C., Chen, Z., 2013. Improvements to the OMI near-UV aerosol algorithm using A-train CALIOP and AIRS observations. Atmospheric Measurement Techniques 6, 3257-3270. https://doi.org/10.5194/amt-6-3257-2013

Torres, O., Tanskanen, A., Veihelmann, B., Ahn, C., Braak, R., Bhartia, P.K., Veefkind, P., Levelt, P., 2007. Aerosols and surface UV products form Ozone Monitoring Instrument observations: An overview. Journal of Geophysical Research Atmospheres 112, D24S47. https://doi.org/10.1029/2007JD008809

Vinoj, V., Rasch, P.J., Wang, H., Yoon, J.H., Ma, P.L., Landu, K., Singh, B., 2014. Short-term modulation of Indian summer monsoon rainfall by West Asian dust. Nature Geoscience 7, pages 308–313. https://doi.org/10.1038/ngeo2107

Wang, H., Shi, G.Y., Zhu, J., Chen, B., Che, H.Z., Zhao, T.L., 2013. Case study of longwave contribution to dust radiative effects over East Asia. Chinese Science Bulletin 58, 3673-3681. https://doi.org/10.1007/s11434-013-5752-z

Wang, W., Sheng, L., Jin, H., Han, Y., 2015. Dust aerosol effects on cirrus and altocumulus clouds in Northwest China. Journal of Meteorological Research 29(5), 793–805. https://doi.org/10.1007/s13351-015-4116-9

Winker, D.M., Hunt, W.H., McGill, M.J., 2007. Initial performance assessment of CALIOP. Geophysical Research Letters 34: L19803. https://doi.org/10.1029/2007GL030135

Yadav, R., Sahu, L.K., Beig, G., Tripathi, N., Jaaffrey, S.N.A., 2017. Ambient particulate matter and carbon monoxide at an urban site of India: Influence of anthropogenic emissions and dust storms. Environmental Pollution 225, 291 – 303. https://doi.org/10.1016/j.envpol.2017.01.038

Young, S.A., Vaughan, M.A., 2009. The retrieval of profiles of particulate extinction from cloud-aerosol lidar infrared pathfinder satellite observations (CALIPSO) data: Algorithm description. Journal of Atmospheric and Oceanic Technology 26, 1105–1119. https://doi.org/10.1175/2008JTECHA1221.1

Yu, X., Kumar, K.R., Lü, R., Ma, J., 2016. Changes in column aerosol optical properties during extreme haze-fog episodes in January 2013 over urban Beijing. Environmental Pollution 210, 217–226. https://doi.org/10.1016/j.envpol.2015.12.021

Zege, E.P., Ivanov, A.P., Katsev, I.L., 1991. Image Transfer Through a Scattering Medium. Springer-Verlag, New York.

Zhang, Y., Li, Z., Zhang, Y., Li, D., Qie, L., Che, H., Xu, H., 2017. Estimation of aerosol complex refractive indices for both fine and coarse modes simultaneously based on AERONET remote sensing products. Atmospheric Measurement Techniques 10, 3203–3213. https://doi.org/10.5194/amt-10-3203-2017

Zhao, T.X.P., Yu, H., Laszlo, I., Chin, M., Conant, W.C., 2008. Derivation of component aerosol direct radiative forcing at the top of atmosphere for clear-sky oceans. Journal of Quantitative Spectroscopy and Radiative Transfer 109(7), 1162-1186. https://doi.org/10.1016/j.jqsrt.2007.10.006

Zhou, Y., Savijärvi, H., 2014. The effect of aerosols on long wave radiation and global warming. Atmospheric Research 135–136, 102–111. https://doi.org/10.1016/j.atmosres.2013.08.009

Assessment of two severe dust storm characteristics over Indo – Gangetic Basin and their implications: a case study

Shani Tiwari[1,2#], Akhilesh Kumar[1], Vineet Pratad[1], A. K. Singh[1,3#]

[1]*Atmospheric Research Laboratory, Department of Physics Banaras Hindu University, Varanasi, India, 221005*

[2]*Now at Environmental Research Institute, Shandong University, China*

[3]*DST - Mahamana Centre of Excellence in Climate Change Research, Banaras Hindu University, Varanasi, India.*

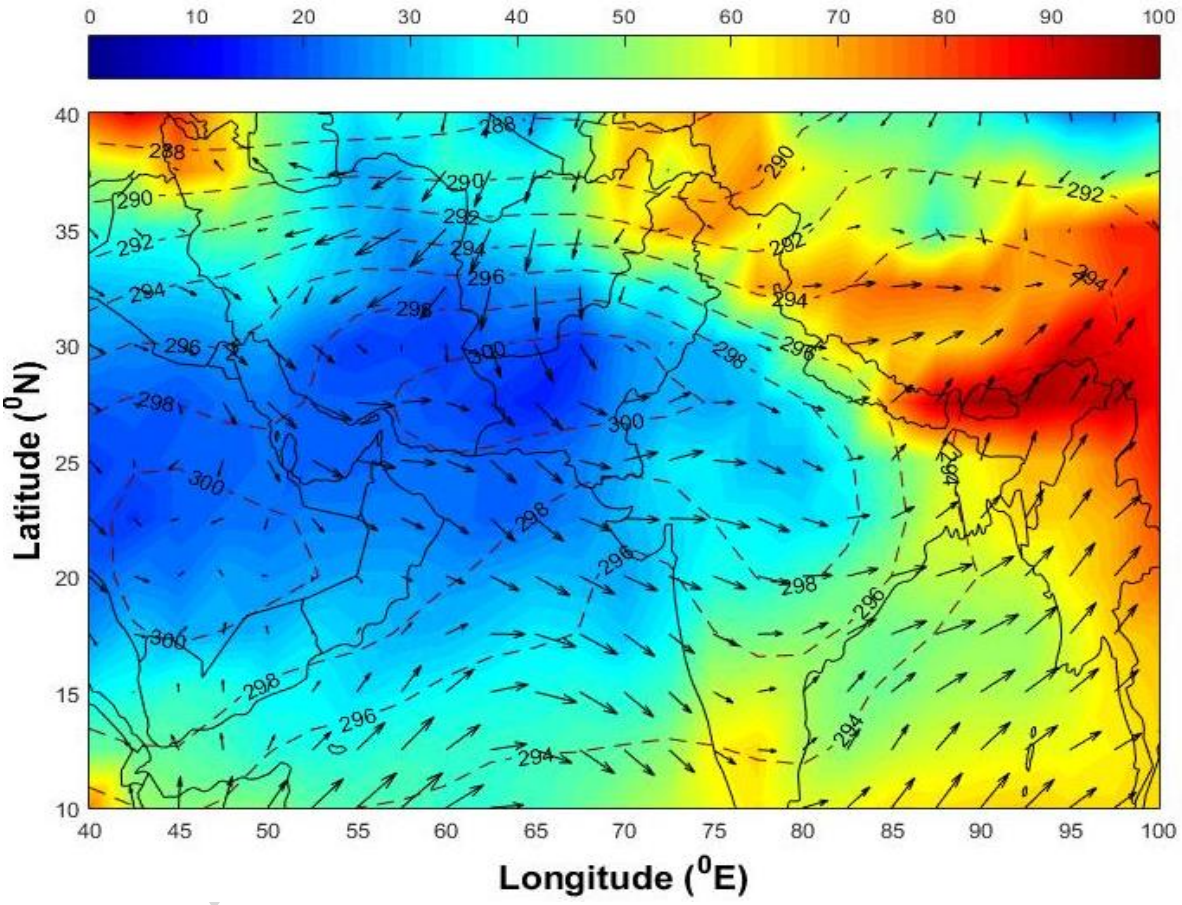

Figure 1. Synoptic meteorological conditions derived from NCEP-reanalysis data at850 hPa pressure level over the Indian subcontinent during the pre-monsoon period of the year 2018.

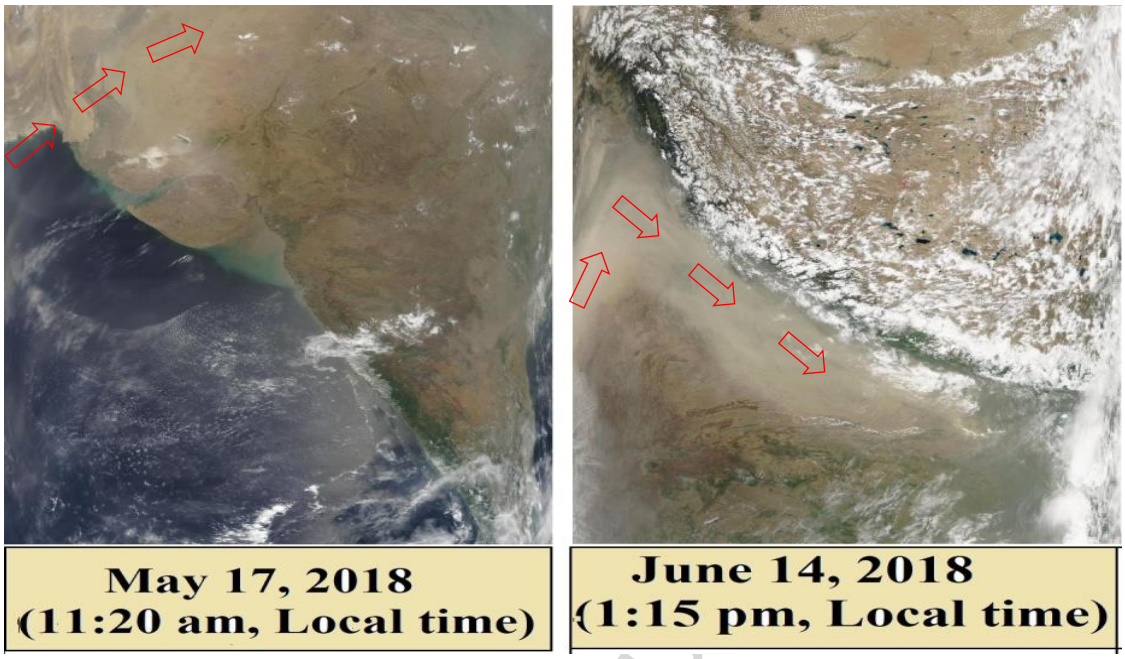

Figure 2. *MODIS TERRA and AQUA images showing long range transport of dust storms. The white colour exhibits clouds. The dust is shown in pale beige colour.* ***Source:*** *http://rapidfire.sci.gsfc.nasa.gov.*

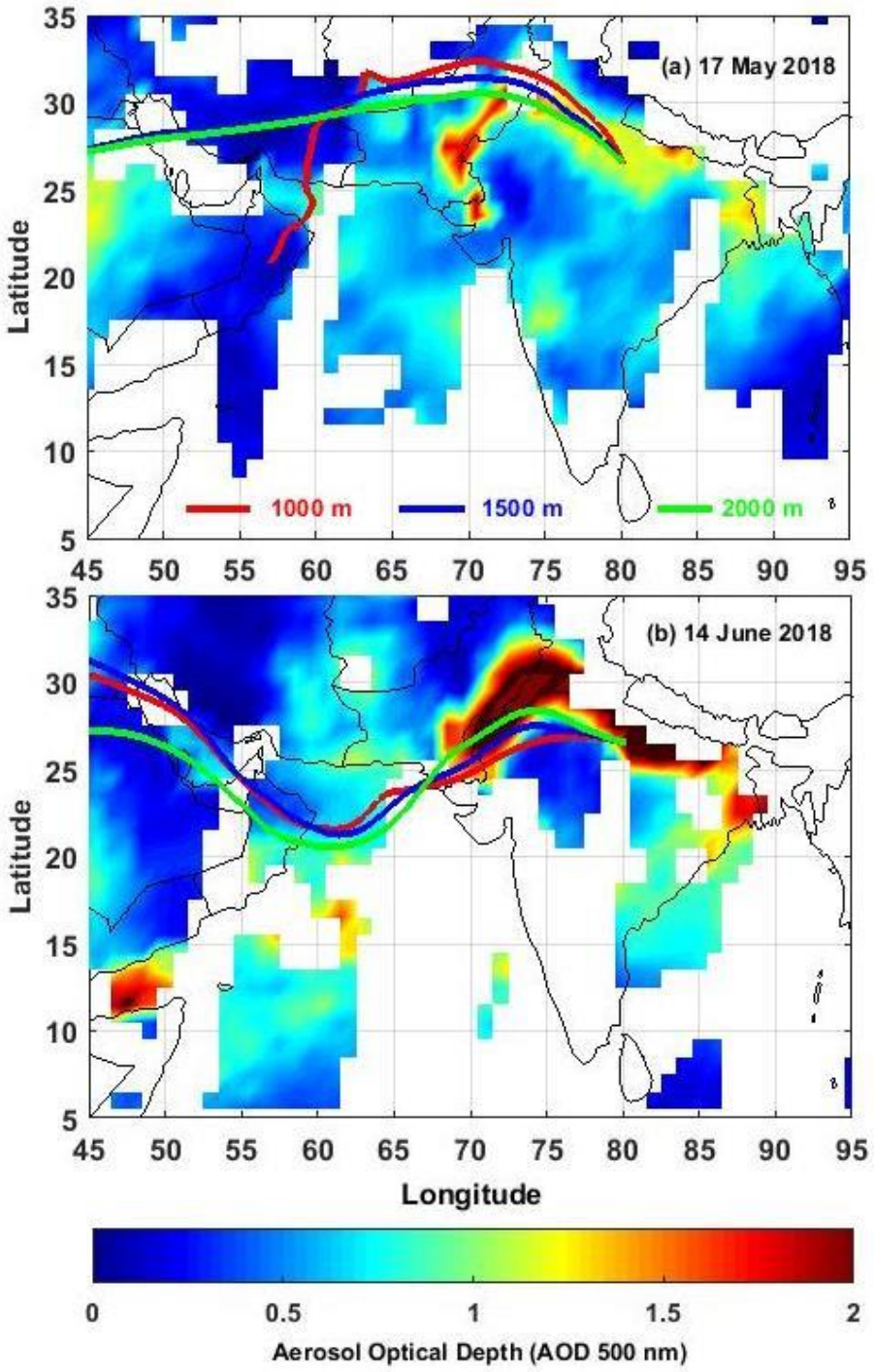

Figure 3. *MODIS terra aerosol optical depth during dust event days, over Indian subcontinent and surrounding regions on (a) 17 May 2018 and (b) 14 June 2018. The colour lines show the 5-days air mass back trajectory over Kanpur station at three different altitude i.e. 1000 m (red), 1500 m (blue) and 2000 m (green).*

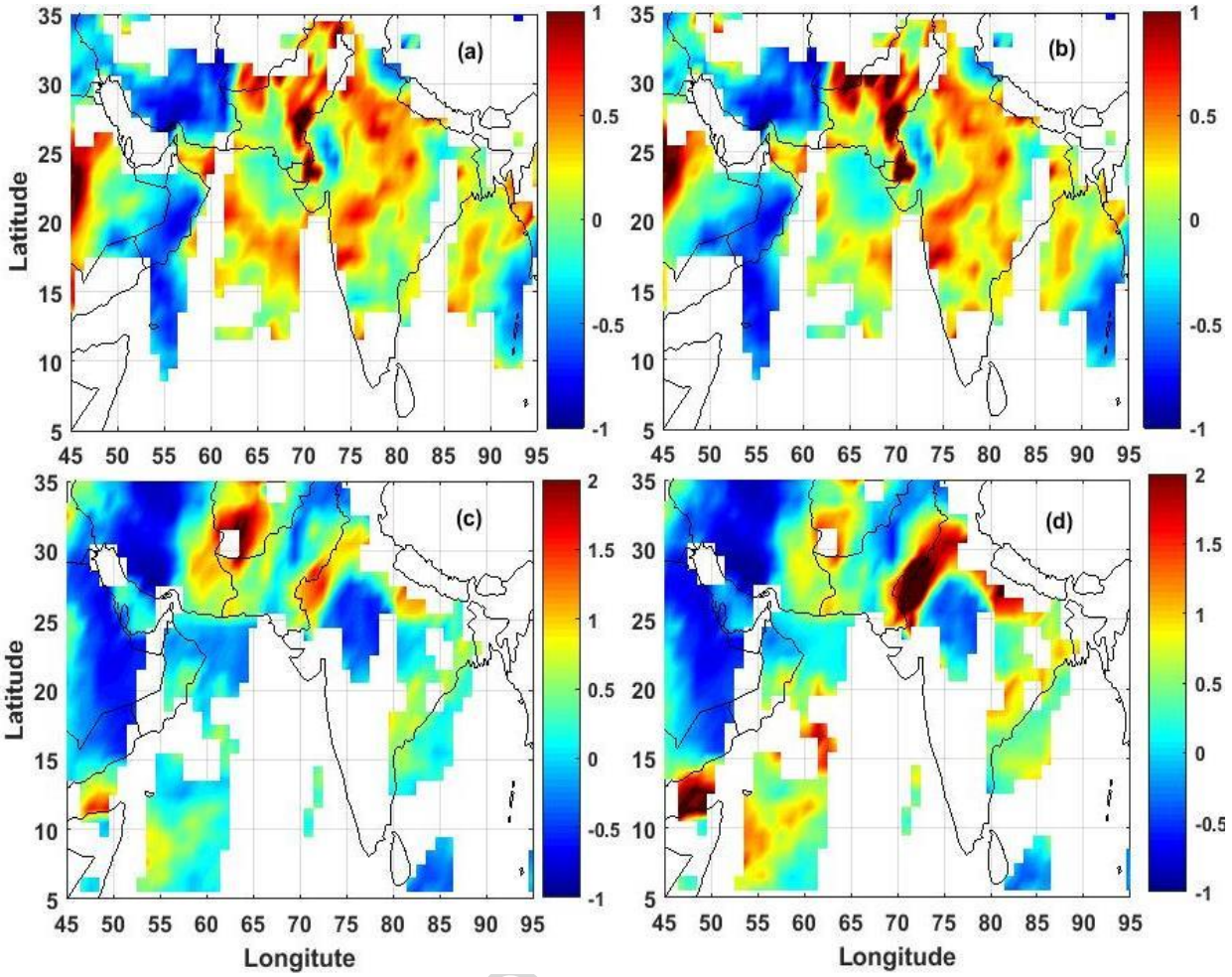

Figure 4. *Spatial distribution of enhancement factor (EF) for aerosol optical depth for the months May (a) and June (c) and on pre-monsoon loading (c) and (d).*

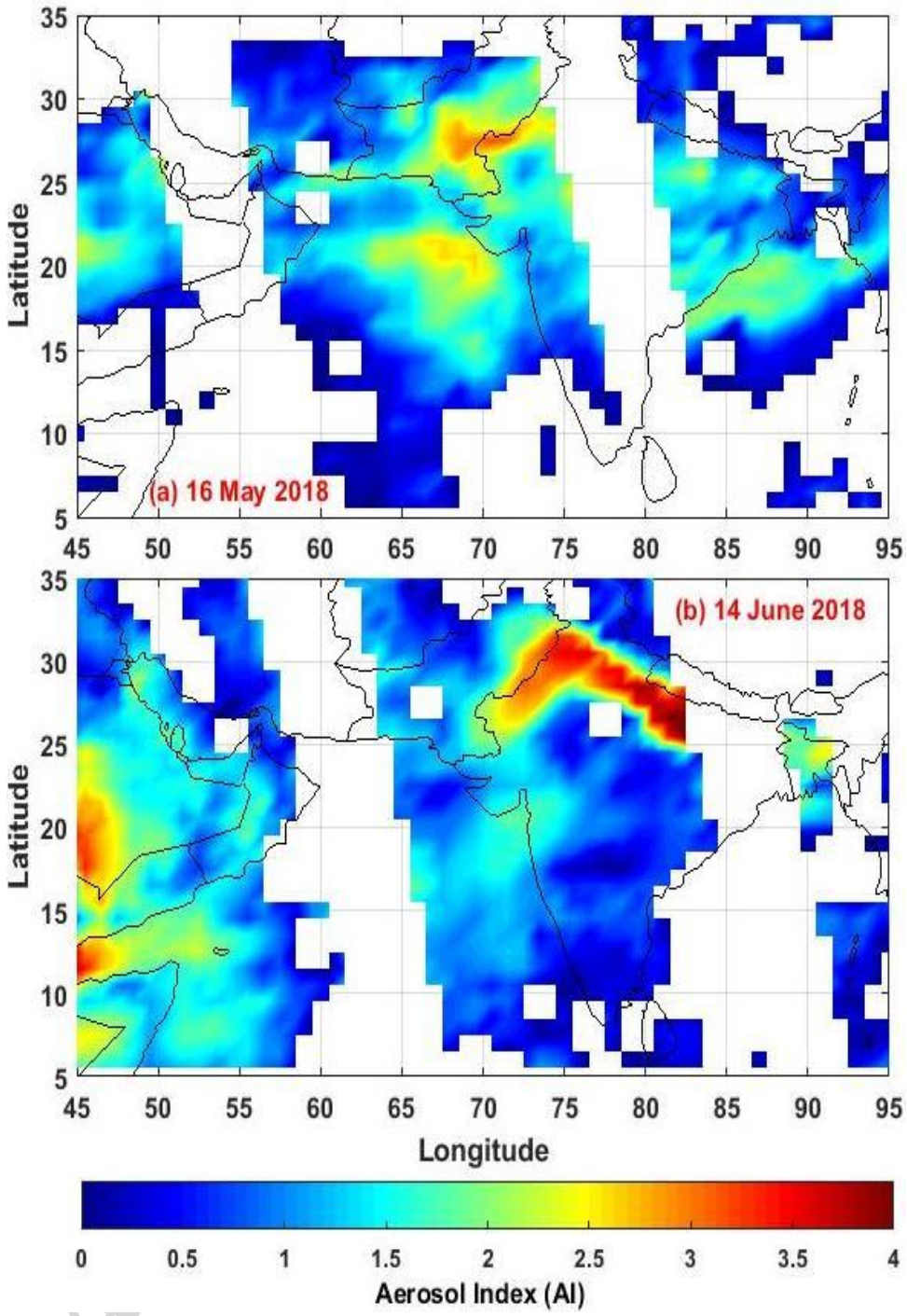

Figure 5. *Spatial distribution of Aerosol Index (AI) during dust event days, over Indian subcontinent and its surrounding regions on (a) 17 May 2018 and (b) 14 June 2018.*

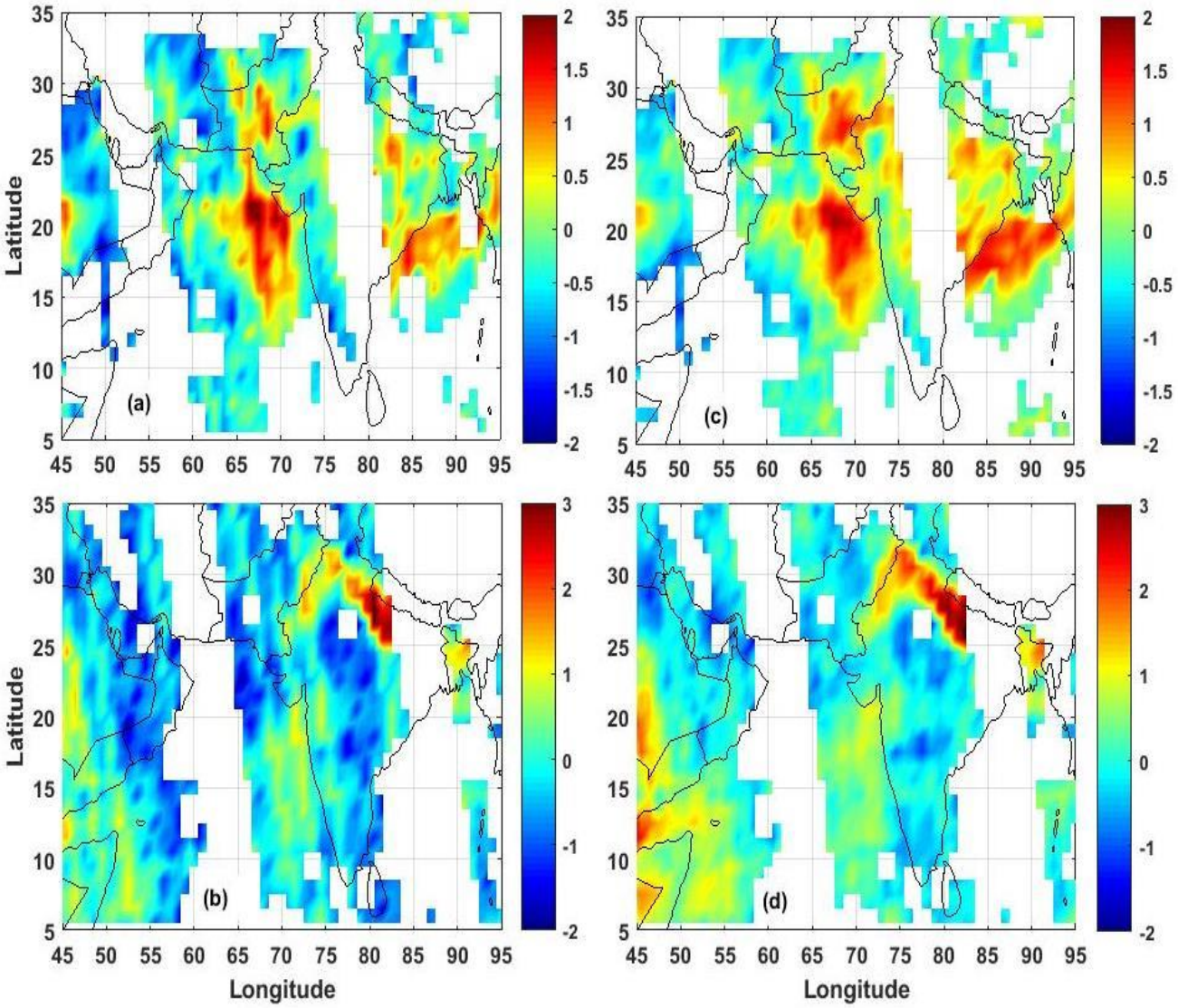

Figure 6. *Spatial distribution of enhancement factor (EF) for aerosol index loading for the months May (a) and June (c) and on pre-monsoon loading (c) and (d).*

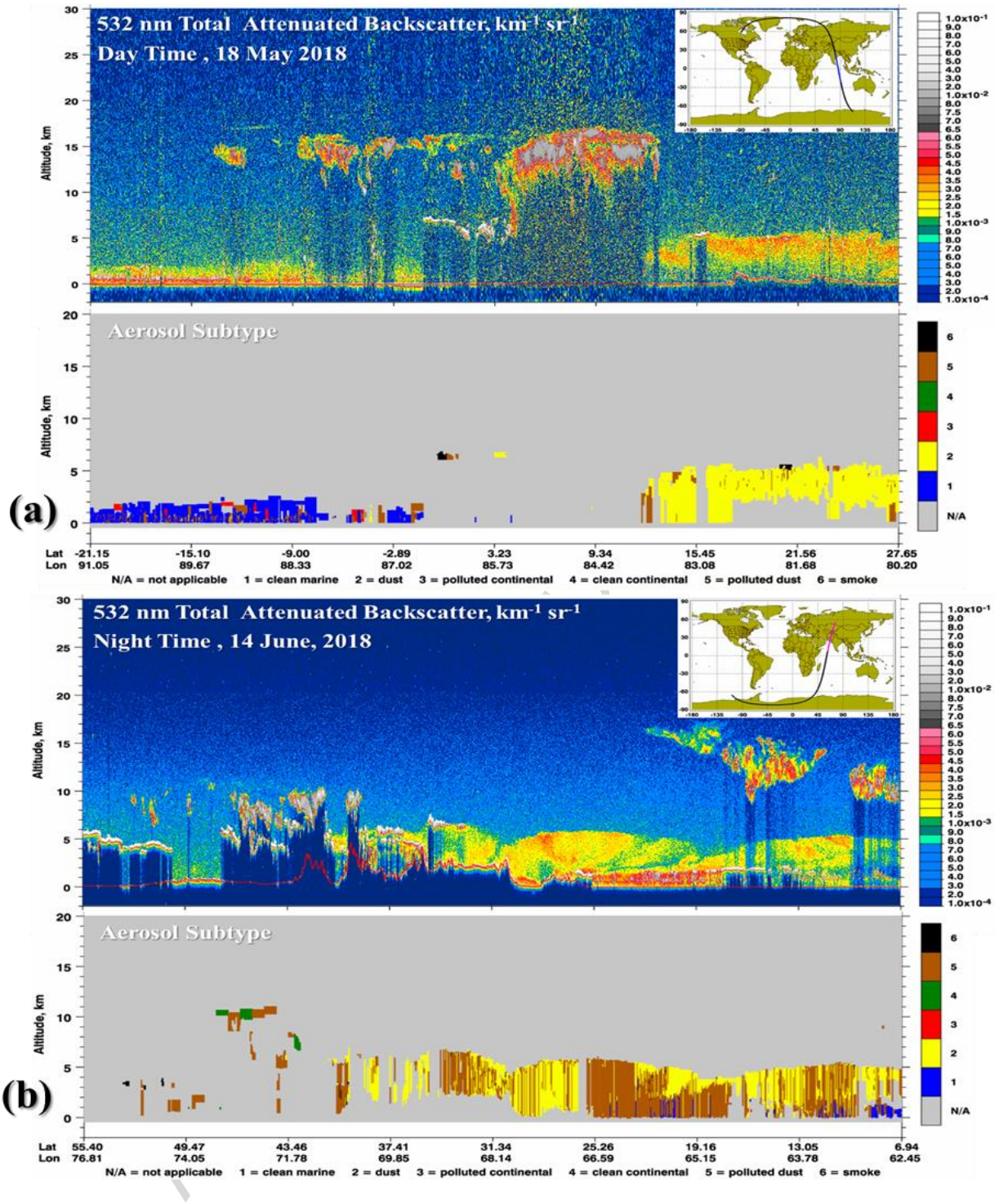

Figure 7: CALIPSO total attenuated backscatter ($km^{-1}sr^{-1}$) and aerosol types over IGB during two intense dust storms (a) 18 May 2018 and (b) 14 June 2018.

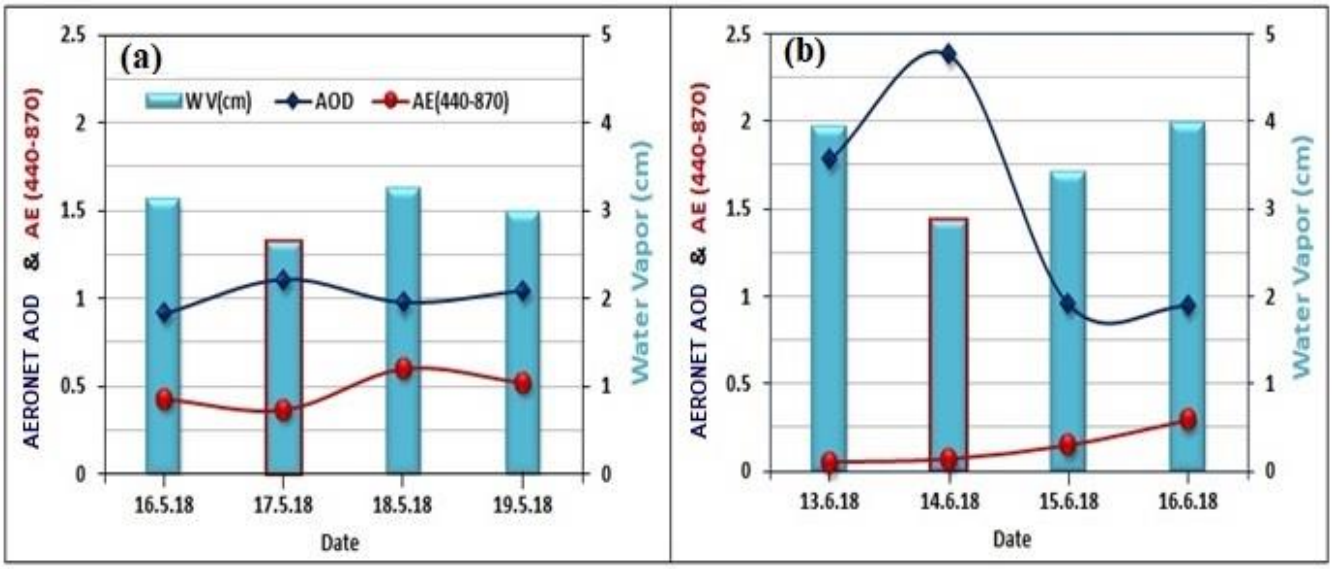

Figure 8. *Day to day variation of AOD (500 nm), Angstrom Exponent ($AE_{440-870\ nm}$) and water vapour during the dust storm events in* (a) May, 2018 and (b) June, 2018.

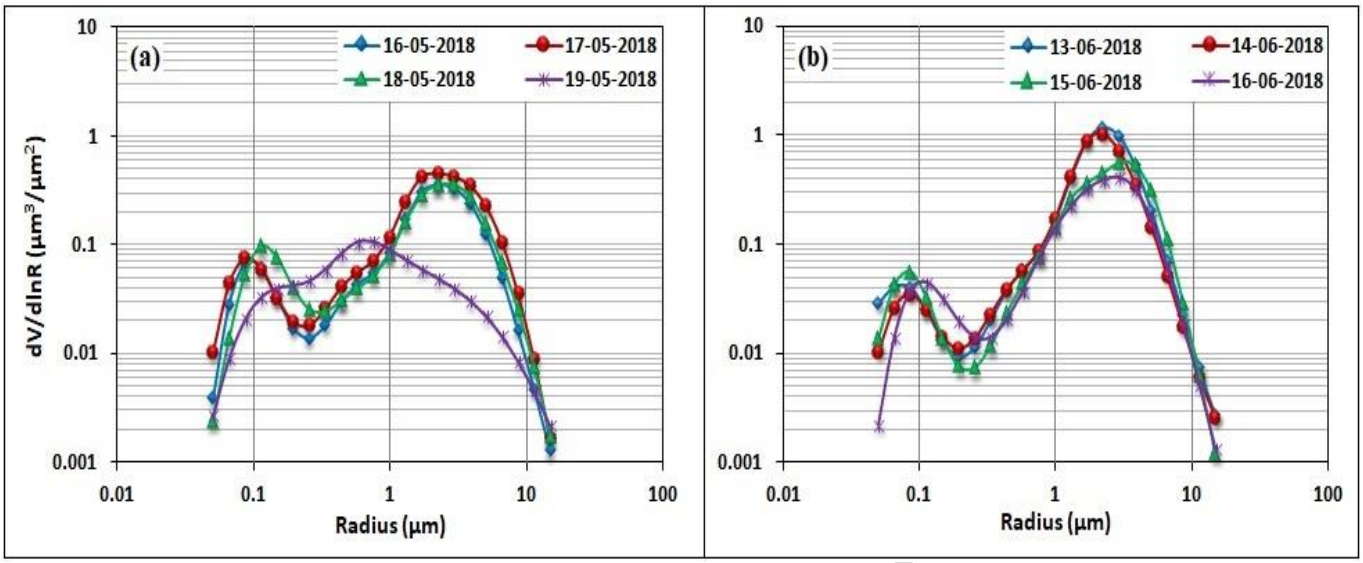

Figure 9. *Aerosol volume size distribution for 22 bins between 0.05 and 15 µm, during the dust events in (a) May and (b) June, 2018.*

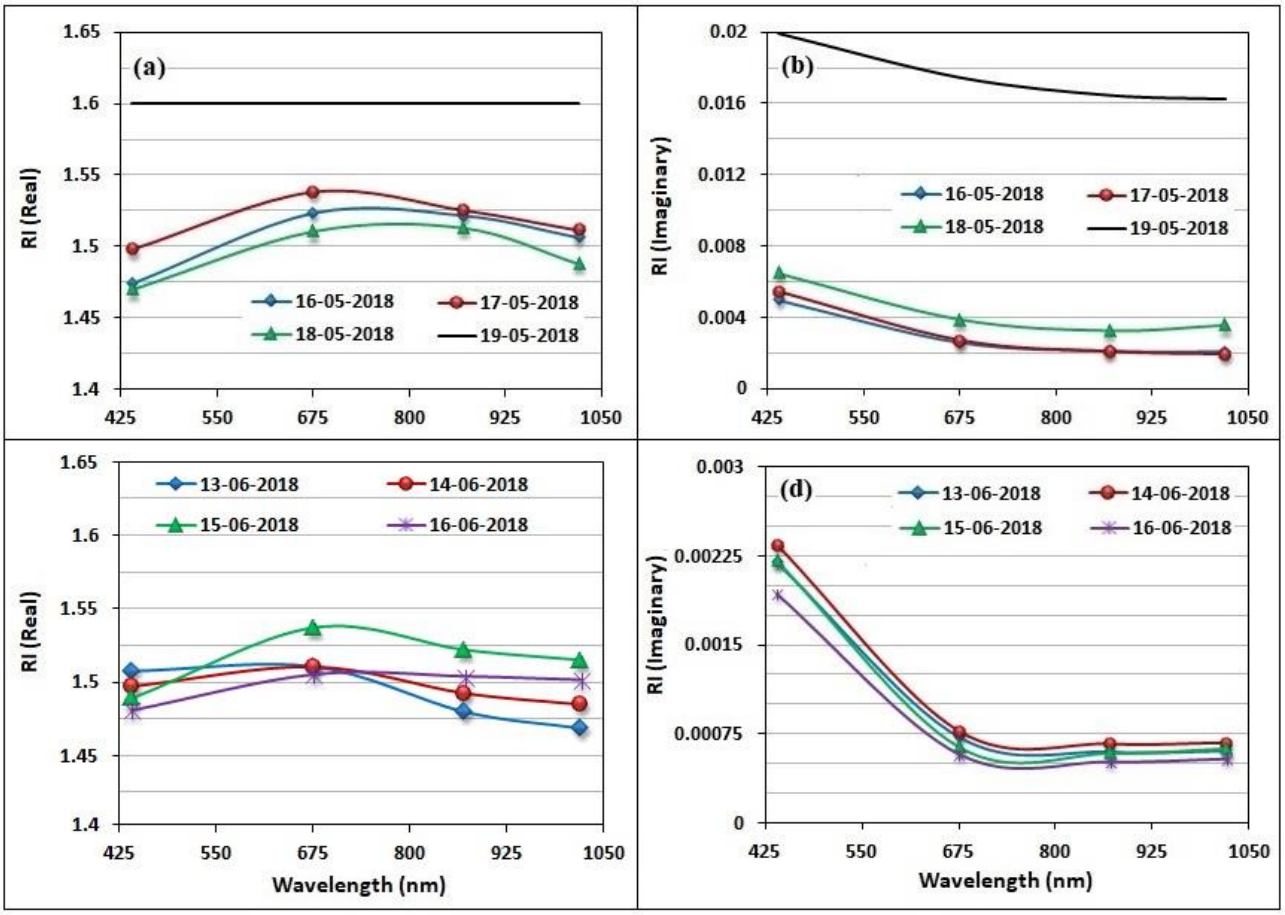

Figure 10. *Spectral variation of real and imaginary refractive index (RI) during the dust storm events in* May, 2018 ((a) and (b)) and in June, 2018 ((c), (d)).

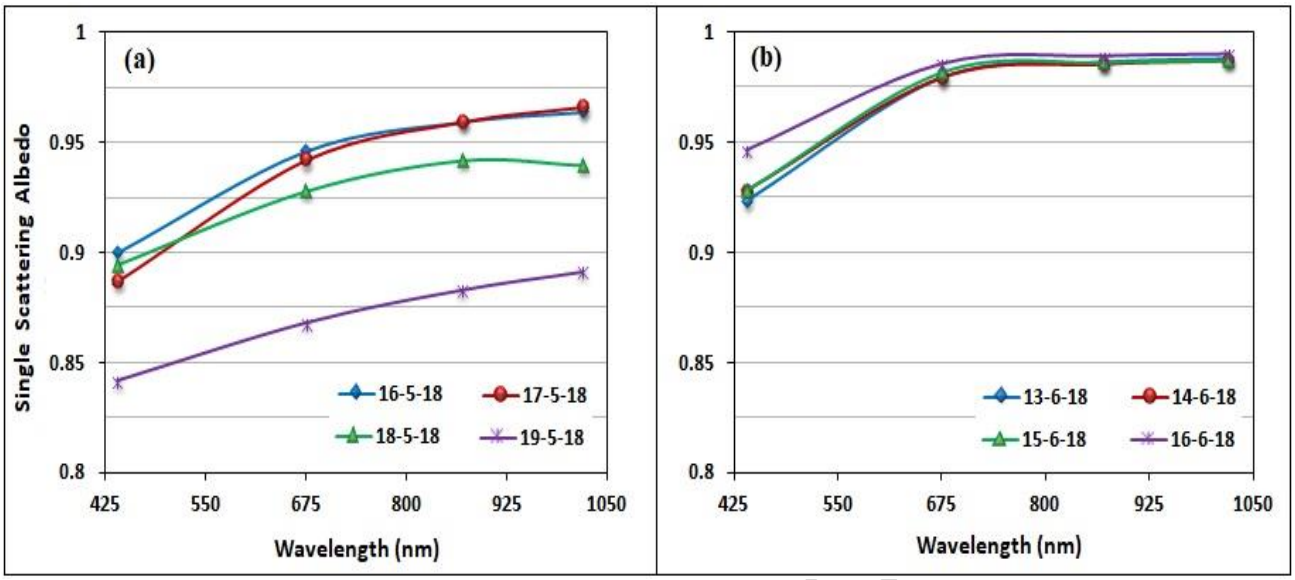

Figure 11. *Spectral variation of single scattering albedo (SSA) during the dust storm events* (a) in May and (b) in June 2018.

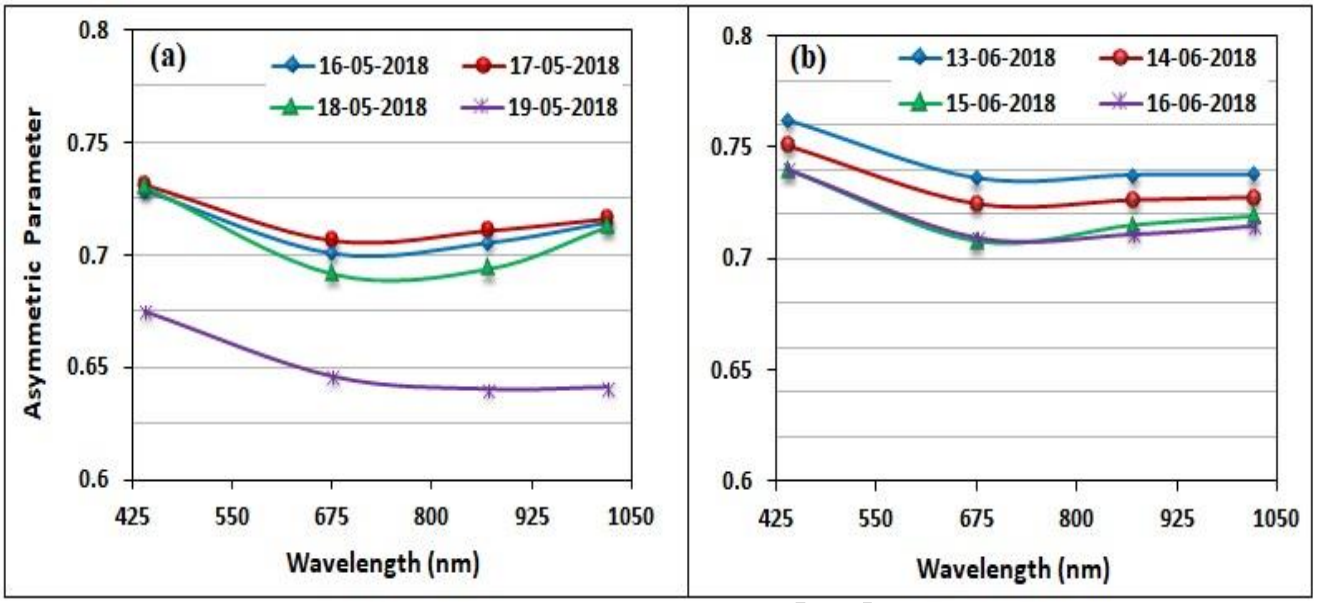

Figure 12. Spectral variation of AERONET asymmetric parameter (AP) during the dust events (a) in May and (b) in June 2018.

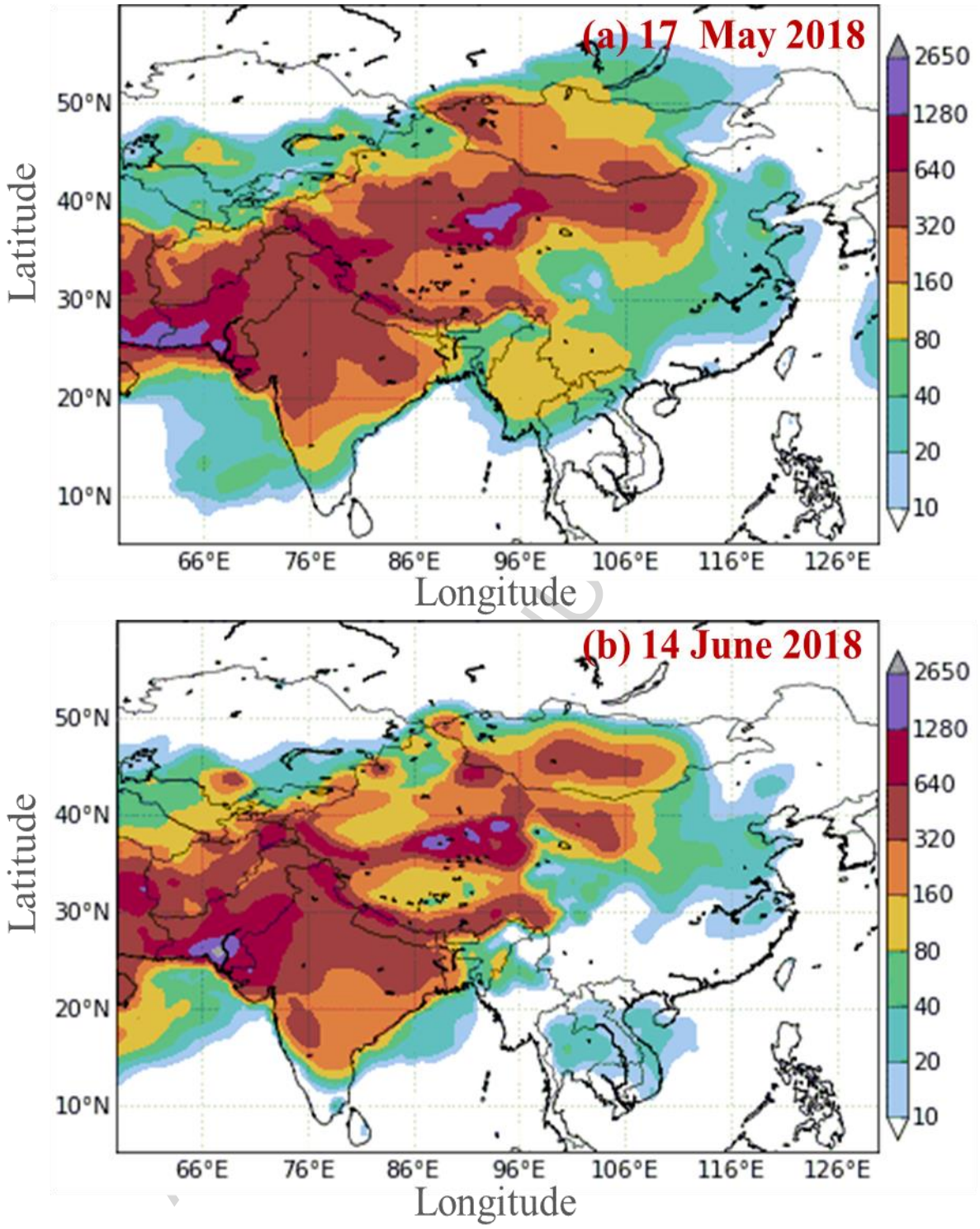

Figure 13. BSC-DREAM8b model-estimated surface dust concentration (μg/m^3) at 12 hrs. UTC over Indian subcontinent and its surrounding region on (a) 17 May 2018 and (b) 14 June 2018.

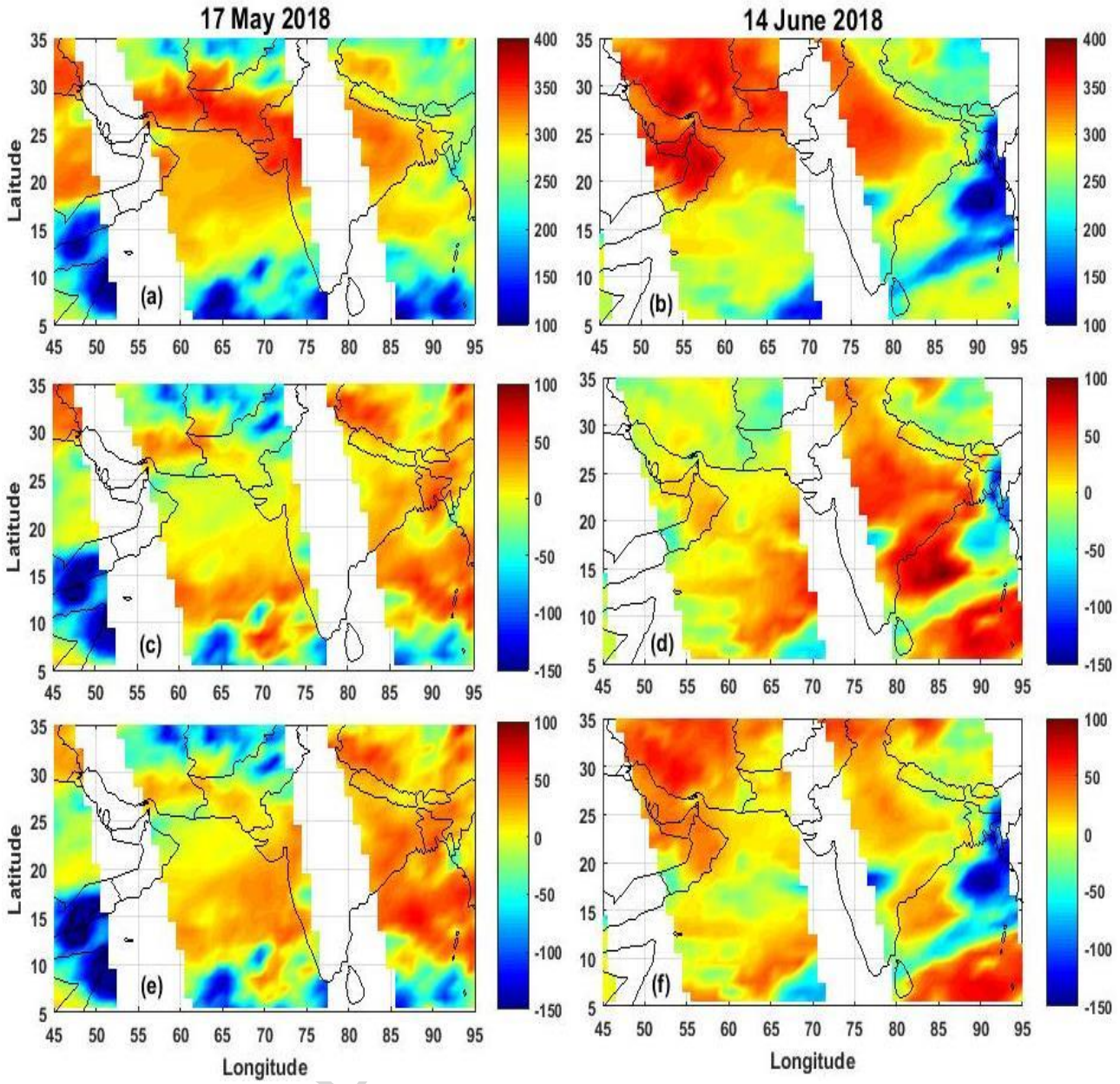

Figure 14. Spatial distribution of outgoing long wave radiation (OLR) during two dust events i.e. (a) on 17 May 2018 and (b) on 14 June 2018.The impact of dust storm on OLR on monthly (c) & (d) as well as seasonal basis (e) & (f).

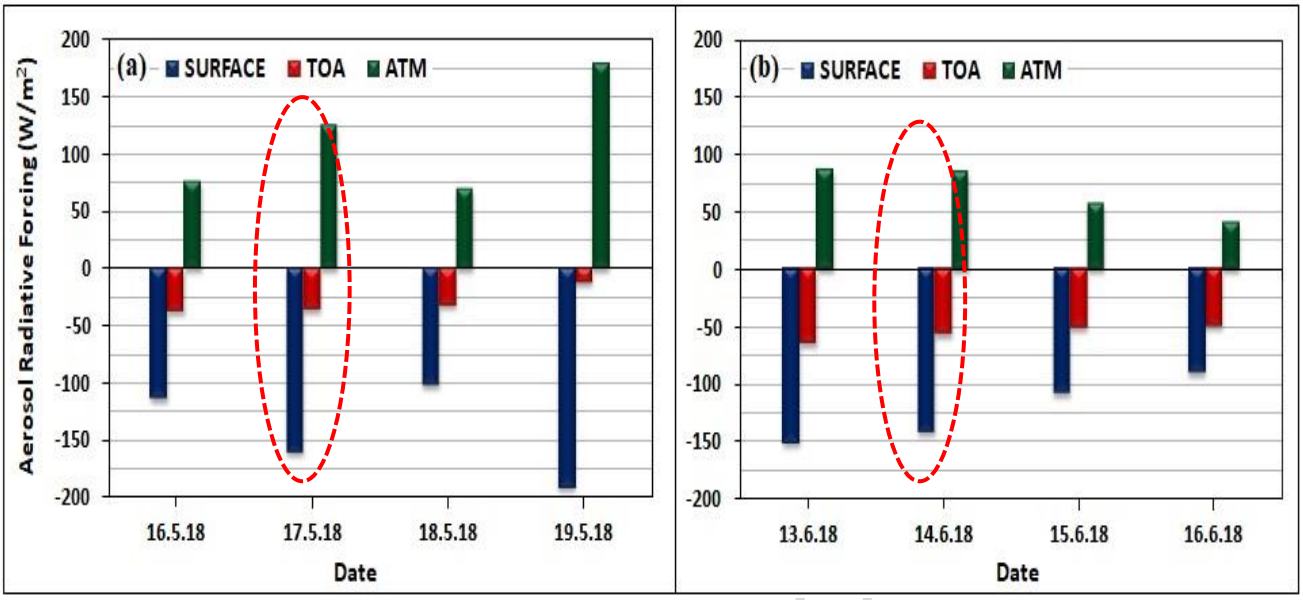

Figure 15. Variation of Atmospheric radiative forcing (ARF) over Kanpur during two dust event events occurred in (a) May 2018 and (b) in June 2018.

Date	Aerosol parameters during the dust storm events								
	AOD (500nm)	AE(440 – 870 nm)	WV (cm)	FMF (500 nm)	AAE (440 – 870 nm)	RRI (675 nm)	IRI (675nm)	SSA (440 nm)	AP (675 nm)
2018/05/16	0.92	0.429	3.12	0.33	1.75	1.52	0.0026	0.90	0.70
2018/05/17	**1.11**	**0.366**	**2.63**	**0. 30**	**1.88**	**1.54**	**0.0027**	**0.89**	**0.71**
2018/05/18	0.98	0.603	3.25	0.42	1.54	1.51	0.0039	0.89	0.69
2018/05/19	1.04	0.522	2.97	0.37	0.96	1.60	0.0175	0.84	0.65
2018/6/13	1.79	0.048	3.95	0.13	2.63	1.51	0.00073	0.92	0.74
2018/6/14	**2.38**	**0.067**	**2.87**	**0.14**	**2.56**	**1.51**	**0.00077**	**0.93**	**0.72**
2018/6/15	0.96	0.147	3.42	0.18	2.67	1.54	0.00064	0.93	0.71
2018/6/16	0.95	0.294	3.98	0.25	2.67	1.51	0.00063	0.95	0.71

Table 1: Day to day variability of aerosol parameters and water vapour (WV) over Kanpur during the dust event days.

Date	Aerosol volume size distribution parameters							
	V_F	R_{efff}	VMR_f	σ_f	V_C	R_{effC}	VMR_C	σ_C
2018/05/16	0.069	0.112	0.128	0.548	0.485	1.905	2.272	0.577
2018/05/17	**0.083**	**0.109**	**0.128**	**0.598**	**0.694**	**1.959**	**2.367**	**0.603**
2018/05/18	0.093	0.131	0.145	0.479	0.503	1.996	2.400	0.589
2018/05/19	0.079	0.177	0.208	0.55	0.174	0.993	1.262	0.769
2018/6/13	0.081	0.099	0.121	0.692	1.250	2.001	2.260	0.478
2018/6/14	**0.048**	**0.119**	**0.144**	**0.635**	**1.076**	**1.916**	**2.218**	**0.522**
2018/6/15	0.053	0.097	0.112	0.583	0.780	2.072	2.483	0.583
2018/6/16	0.052	0.123	0.140	0.527	0.603	1.933	2.298	0.575

Table 2: Aerosol volume size distribution parameters during dust events over Kanpur. Vf and Vc are the volume concentration (in $\mu m^3 \mu m^{-2}$) of fine and coarse particles, respectively. R_{efff} and R_{effc} are the effective radii (in μm) of fine and coarse modes, respectively. VMR_f and VMR_c are the volume

median radius (in μm) of fine and coarse modes, respectivelywhile σ_f and σ_c are the geometric standard deviation of fine and coarse modes, respectively.

Date	**$ARF_{SRF}(Wm^{-2})$**	**$ARF_{TOA}(Wm^{-2})$**	**$ARF_{ATM}(Wm^{-2})$**	**HR ($Kday^{-1}$)**
2018/5/16	-114.25	-37.69	76.56	1.66
2018/5/17	**-160.45**	**-36.06**	**124.40**	**2.70**
2018/5/18	-101.89	-32.20	69.69	1.51
2018/5/19	-191.56	-12.34	179.22	3.88
2018/6/13	-151.44	-64.68	86.76	1.88
2018/6/14	**-141.45**	**-56.51**	**84.94**	**1.84**
2018/6/15	-108.11	-50.96	57.15	1.24
2018/6/16	-90.26	-49.14	41.12	0.89

Table 3: Aerosol Radiative forcing at SRF, TOA, ATM in (Wm^{-2}) and heating rate ($Kday^{-1}$) during the dust events. The bold blue colourshow values on maximum intensity of the dust storm.

Highlights:

- Modification in aerosol optical & physical properties over IGB during major dust storms of 2018.
- Vertical distribution of dust plumes up to ~5 km over Ganges Basin.
- Significant radiative forcing & atmospheric heating during two dust events over Kanpur.